Attribution of stratospheric and tropospheric ozone changes between 1850 and 2014 in CMIP6 models

Guang Zeng[1], N. Luke Abraham[2,3], Alexander T. Archibald[2,3], Susanne E. Bauer[4,5], Makoto Deushi[6], Louisa K. Emmons[7], Paul T. Griffiths[2,3], Birgit Hassler[8], Larry W. Horowitz[9], James Keeble[2,3], Michael J. Mills[7], Olaf Morgenstern[1], Lee T. Murray[10], Vaishali Naik[9], Fiona M. O'Connor[11], Naga Oshima[6], Lori T. Sentman[9], Simone Tilmes[7], Kostas Tsigaridis[4,5], Jonny H. T. Williams[1], and Paul J. Young[12,13]

[1]National Institute of Water and Atmospheric Research (NIWA), Wellington, New Zealand
[2]National Centre for Atmospheric Science, U.K.
[3]Department of Chemistry, University of Cambridge, Cambridge, U.K.
[4]NASA Goddard Institute for Space Studies (GISS), New York, NY, USA
[5]Center for Climate Systems Research, Columbia University, New York, NY, USA
[6]Meteorological Research Institute (MRI), Tsukuba, Japan
[7]National Center for Atmospheric Research (NCAR), Boulder, CO, USA
[8]Deutsches Zentrum für Luft- und Raumfahrt (DLR), Institut für Physik der Atmosphäre, Oberpfaffenhofen, Germany
[9]Geophysical Fluid Dynamics Laboratory (GFDL), National Oceanic and Atmospheric Administration, Princeton, NJ, USA
[10]University of Rochester, Rochester, NY, USA
[11]Hadley Centre, Met Office, Exeter, UK
[12]Lancaster Environment Centre, Lancaster University, Lancaster, UK
[13]Centre of Excellence in Environmental Data Science, Lancaster University, Lancaster, UK

Key Points:

- Changes in ozone-depleting substances, greenhouse gases, and ozone precursors significantly impact stratospheric and tropospheric ozone.
- Tropospheric ozone contributes increasingly importantly to total column ozone changes.

Corresponding author: Guang Zeng, guang.zeng@niwa.co.nz

- Changes in stratospheric ozone and circulation significantly impact tropospheric ozone through stratosphere-troposphere exchange.

Abstract

We quantify the impacts of halogenated ozone-depleting substances (ODSs), methane, N_2O, CO_2, and short-lived ozone precursors on total and partial ozone column changes between 1850 and 2014 using CMIP6 Aerosol and Chemistry Model Intercomparison Project (AerChemMIP) simulations. We find that whilst substantial ODS-induced ozone loss dominates the stratospheric ozone changes since the 1970s, the increases in short-lived ozone precursors and methane lead to increases in tropospheric ozone since the 1950s that make increasingly important contributions to total column ozone (TCO) changes. Our results show that methane impacts stratospheric ozone changes through its reaction with atomic chlorine leading to ozone increases, but this impact will decrease with declining ODSs. The N_2O increases mainly impact ozone through NO_x-induced ozone destruction in the stratosphere, having an overall small negative impact on TCO. CO_2 increases lead to increased global stratospheric ozone due to stratospheric cooling. However, importantly CO_2 increases cause TCO to decrease in the tropics. Large interannual variability obscures the responses of stratospheric ozone to N_2O and CO_2 changes. Substantial inter-model differences originate in the models' representations of ODS-induced ozone depletion. We find that, although the tropospheric ozone trend is driven by the increase in its precursors, the stratospheric changes significantly impact the upper tropospheric ozone trend through modified stratospheric circulation and stratospheric ozone depletion. The speed-up of stratospheric overturning (i.e. decreasing age of air) is driven mainly by ODS and CO_2 increases. Changes in methane and ozone precursors also modulate the cross-tropopause ozone flux.

Plain Language Summary

Overhead ozone absorbs harmful sunlight, protecting life on Earth. Due to human activities since the 19^{th} century, emissions of greenhouse gases (GHGs) and ozone-depleting substances (ODSs) containing chlorine and bromine have profoundly affected stratospheric ozone. Near the Earth's surface, ozone has increased substantially leading to worsened air quality. In this study, we use Earth System models to interactively assess the roles of ODSs, ozone-forming pollutants, and GHGs including methane, carbon dioxide, and nitrous oxide on ozone changes from the surface to the upper stratosphere. While substantial reductions in stratospheric ozone due to ODSs occurred since the 1970s, the lower-atmospheric ozone increases due to industrial pollution have countered this decrease. In-

creases in GHGs impact stratospheric ozone with various positive and negative effects, and complicating this, their impacts vary with ODS levels in the atmosphere. We have also assessed the impact of changes in stratospheric ozone and circulation on lower-atmospheric ozone through stratosphere-troposphere exchange, and find that ODS increases produce a decrease in net downward transport of ozone, offset by increases in methane causing an increased net flux of ozone, and compounded by industrial pollution with ozone precursors driving a decreasing net flux of ozone from the stratosphere.

1 Introduction

Since preindustrial (PI) times, anthropogenic forcing has driven considerable ozone changes, both in the stratosphere and the troposphere. Stratospheric ozone prevents harmful ultraviolet radiation from reaching the Earth's surface. Ozone results from natural photochemical production and destruction cycles in the stratosphere. Stratospheric ozone can be transported into the troposphere, contributing to background tropospheric ozone that is in balance with chemical destruction and deposition to the surface. However, both stratospheric and tropospheric ozone have been perturbed by anthropogenic influences. The most significant impact on stratospheric ozone is from halogenated ozone-depleting substances (ODSs) that have damaged the ozone layer since the 1970s (Farman & Shanklin, 1985; Solomon, 1999). In the troposphere, emissions of ozone precursors, including nitrogen oxides (NO_x=NO+NO_2), methane, and non-methane volatile organic compounds, have led to substantial ozone increases since PI times (Volz & Kley, 1988; Gaudel et al., 2018). Tropospheric ozone is a greenhouse gas (GHGs) and air pollutant harmful to human health and vegetation.

In addition to ODSs, increases in long-lived GHGs (especially CO_2, N_2O, and CH_4) also impact stratospheric ozone chemically and dynamically (Fleming et al., 2011; Reader et al., 2013; Revell et al., 2015; Butler et al., 2016). Methane is an ozone precursor in the troposphere promoting ozone production in the presence of NO_x. In the stratosphere, methane affects ozone in several ways (Brasseur & Solomon, 1984): (1) Increasing methane leads to water vapor production in the stratosphere which enhances the ozone loss through HO_x-cycle. This process is more important in the upper stratosphere and the mesosphere. (2) Increasing H_2O leads to cooling in the stratosphere that slows down ozone loss; this process is more pronounced in the middle stratosphere (Fleming et al., 2011). (3) Methane reacts with free chlorine (Cl) to produce HCl, and this deactivation of Cl leads to reduced

ozone depletion, which can result in a significant impact on stratospheric ozone whilst the ODS loading is high (Fleming et al., 2011; Revell et al., 2012; Reader et al., 2013).

The increase of N_2O mainly impacts ozone through NO_x-induced ozone destruction in the stratosphere (Crutzen, 1970). However, in a high Cl loading environment, the available NO_2 will be reduced by forming $ClONO_2$, therefore reducing the ozone-destruction efficiency (Portmann et al., 2012; Stolarski & Waugh, 2015; Revell et al., 2015). CO_2-induced stratospheric cooling can slow down the ozone destruction rate there (e.g. Haigh & Pyle, 1979; Chipperfield & Feng, 2003; Oman et al., 2010), therefore leading to an ozone increase. CO_2 increases also result in changes in stratospheric circulation and a speedup of the Brewer-Dobson circulation (Butchart & Scaife, 2001; Butchart, 2014) that enhances the stratosphere-troposphere exchange. The dynamical changes in the lower stratosphere and the upper troposphere, e.g., the rise of the tropopause, could modify the vertical ozone distribution in that region (Oberländer-Hayn et al., 2016). Changes in stratospheric ozone and circulation can also affect tropospheric ozone through stratosphere-troposphere exchange (STE) (Hegglin, 2009; Zeng et al., 2010).

Past studies have usually assessed the impact of anthropogenic forcing on ozone changes with a focus on either the stratosphere or the troposphere, using a variety of chemistry-climate models. This is partly due to the only recent availability of fully coupled stratosphere-troposphere chemistry-climate models. Fleming et al. (2011) use a 2-dimensional model to study the impact of ODSs, CO_2, N_2O, and methane on changes in the stratosphere between 1850 and 2100. Morgenstern et al. (2018) assess the sensitivity of ozone changes to changes in ODS, N_2O, and methane in Chemistry-Climate Model Initiative Phase 1 (CCMI-1) models using perturbation simulations that cover 1960-2100. They find that while the models agree well in simulating the response of ozone changes to anthropogenic forcings in the middle and upper stratosphere, the agreement is less good in the lower stratosphere and troposphere as some models do not include detailed tropospheric chemistry and dynamical feedbacks challenge this group of models. However, Reader et al. (2013) investigate ozone changes from preindustrial times to the present using a chemistry-climate model, and assessed the influence of changes in ODSs, N_2O, and tropospheric ozone precursors. They find that the increase in lower stratospheric ozone associated with the increase in ozone precursors contribute significantly to the total column ozone. Previously, models used in multi-model simulations of tropospheric ozone changes often did not include an interactive stratosphere (Stevenson et al., 2006), or included models with

variably comprehensive tropospheric and stratospheric chemistry (Young et al., 2013; Iglesias-Suarez et al., 2016). Eyring et al. (2013) document ozone changes and associated climate impacts in the Coupled Model Intercomparison Project Phase 5 (CMIP5) simulations and point out that some large ozone biases exist for individual models with interactive chemistry.

The emergence of fully coupled stratosphere-troposphere chemistry-climate models makes it possible to explore the coupling between stratospheric and tropospheric ozone changes and their responses to anthropogenic forcing more comprehensively. The recently available model simulations from the 6^{th} Coupled Model Intercomparison Project (CMIP6) (Eyring et al., 2016), and specifically from the Aerosol and Chemistry Model Intercomparison Project (AerChemMIP) (Collins et al., 2017), allow us to assess stratospheric and tropospheric ozone changes in response to changes in ODSs, CO_2, N_2O, methane, and ozone precursors between 1850 to 2014. All AerChemMIP models included in this study have interactive stratospheric and tropospheric chemistry. In particular, the contributions of ozone precursors to total column ozone can be assessed in these models.

The subsequent sections are organised as follows: In Section 2, we describe the AerChemMIP model simulations used in this study. In Section 3, we present the impacts of individual forcings on total and partial ozone columns, the responses of global ozone to the forcings, and an attribution of the vertically resolved ozone changes for the periods of 1979-1999 and 2000-2014, respectively. We also examine the impact of stratospheric changes on tropospheric ozone. A summary and conclusions are in Section 4.

2 CMIP6 AerChemMIP simulations, models, and methods

The AerChemMIP is a constituent model intercomparison project of CMIP6. Its purpose is to quantify the impact of aerosols and chemically reactive gases on climate and vice versa (Collins et al., 2017). The reference experiment "histSST" is an atmosphere-only single member experiment with sea-surface temperatures (SSTs) and sea ice concentrations (SIC) taken from a corresponding fully coupled atmosphere-ocean CMIP6 "historical" simulation with anthropogenic forcing covering 1850-2014 (Eyring et al., 2016). Complementing the histSST experiment, a set of perturbation experiments is used to discern the impacts of individual forcings on atmospheric composition. The "historical" simulations have been used in several CMIP6 model comparison studies on past changes in

tropospheric and stratospheric ozone, methane lifetime, and OH (Morgenstern et al., 2020; Stevenson et al., 2020; Griffiths et al., 2021; Keeble et al., 2021). Here, we analyse the AerChemMIP perturbation simulations to assess impacts of ODS, methane, N_2O, CO_2, and ozone precursors (the "near-term climate forcers" (NTCFs) in AerChemMIP) on stratospheric and tropospheric ozone between 1850 and 2014. The models and the AerChemMIP simulations used in this study are listed in Table 1.

In all perturbation simulations, the concentrations or emissions of individual forcers are fixed at their preindustrial levels, except for ODSs that are fixed at their 1950 levels (from 1850 to 1950 the ODSs are invariant in the "historical" scenario). The impact of each forcing on ozone changes is expressed as the difference between the "all forcing" histSST simulation and a corresponding perturbation simulation (Table 2). The time evolution of ozone in each simulation is expressed as a deviation from its average over the period 1850-1900. This experimental design captures only the "fast" atmospheric response to forcing changes, but not any responses involving SST changes due to the individual forcings. As simulations aiming to directly quantify the impact of CO_2 increases are not available in AerChemMIP, we derive the impact of CO_2 as the difference between the histSST simulation and the sum of all single-forcing perturbations assuming that any coupling effects are small (Table 2). The impacts of combined GHGs (methane, CO_2, and N_2O) and long-lived GHGs (LLGHGs: CO_2 and N_2O) can also be derived from available perturbation simulations (Table 2). The effects of other minor GHGs are assumed to be small in this.

We use data from five CMIP6 models (CESM2-WACCM, GFDL-ESM4, MRI-ESM2-0, UKESM1-0-LL, and GISS-E2-1-G), available at the ESGF data archive (https://esgf-node.llnl.gov/search/cmip6/). In "historical" simulations all are fully coupled ocean-atmosphere Earth System models with interactive stratospheric and tropospheric chemistry schemes. More detailed description of the models have been given by Griffiths et al. (2021) and the references therein (cf. Table 1). These models have been evaluated for their suitability for simulating past ozone changes in both the stratosphere and the troposphere (Morgenstern et al., 2020; Morgenstern, 2021; Griffiths et al., 2021; Keeble et al., 2021). All five models have performed histSST, ODS, and ozone precursor perturbation simulations, all models but CESM2-WACCM have also performed methane perturbation simulations, and three models (MRI-ESM2-0, UKESM1-0-LL, and GISS-E2-1-G) have performed all perturbation simulations (Table 1). Among the five models, GISS-E2-1-G exhibits a much

bigger response to volcanic eruptions than the other models (Morgenstern et al., 2020), which leads to an abnormally strong ozone response in the "all forcing" historical simulation. Therefore, we do not include this model in the multi-model ensemble means. However, for completeness we do show the results of its response to individual forcing in the supplement, because the strong response to volcanic eruptions is largely cancelled in comparisons of paired simulations.

In the historical scenario, the greenhouse gases (CO_2, N_2O, and methane) (Meinshausen et al., 2017) all show monotonic increases since 1850 with steeper increases from the 1970s (Figure 1). An exception is CH_4 which plateaued around 2000. The ODSs are represented by equivalent chlorine (Cl_{eq}), i.e. the sum of ODSs weighted with their per-molecule chlorine and bromine contents (where the bromine contribution is scaled by a factor of 60) and shifted by 4 years, to account for transport (Newman et al., 2007). Cl_{eq} shows a sharp rise from the 1950s before declining from the late 1990s. Near-term climate forcers (NTCFs) comprise ozone and aerosol precursors (we also refer to "NTCFs" as "ozone precursors" herein), with emissions of carbon monoxide (CO), nitrogen oxides (NO_x), and biogenic volatile organic compounds all increasing since the pre-industrial period (as shown in Figure 1 of Griffiths et al., 2021). For regression purposes we use the global mean surface ozone value averaged between all five models as a single metric for the overall effect of ozone precursors. Although the GISS-E2-1-G model results are not included in any of the multimodel means, we show the response of ozone changes to forcings in this model for the reason stated above. The global mean surface ozone values are very similar among the five models.

We calculate the total and partial ozone columns using monthly-mean ozone and related fields on the models' native grids. The tropopause is defined using the tropopause pressure output from each model based on the WMO lapse rate definition (REFERENCE), and the tropospheric columns are the integrals of the ozone concentrations below the thus defined tropopause. The changes in vertically resolved distributions of ozone are calculated using the monthly-mean ozone fields interpolated onto a common grid of 39 levels from 1000 to 0.03 hPa.

We use a linear regression approach to assess the response of global ozone changes to the forcings. Following Morgenstern et al. (2018) we express ozone sensitivities to the

various forcing agents as coefficients in least-squares regression fits, e.g.

$$[O_3]_{histSST} = [O_3]_{histSST\text{-}1950HC} + A_0 \Delta Cl_{eq} + \epsilon \quad (1)$$

where $[O_3]_{histSST}$ and $[O_3]_{histSST\text{-}1950HC}$ are timeseries of ozone concentrations from the "all forcing" histSST and the fixed 1950HC perturbation experiments (Table 1), ΔCl_{eq} is the difference in equivalent chlorine between the two experiments, A_0 is the regression fit describing the sensitivity of ozone to ODSs, and ϵ is the error minimized in the fitting process. Analogous formulae hold for the other forcing agents.

3 Results

3.1 Evolution of ozone columns between 1850 and 2014

We compare stratospheric, tropospheric and total-column ozone changes in the histSST simulations (figure 2). Despite some large inter-model differences in TCO (red shading), the MMM TCO is in very good agreement with the observations in all regions and captures the observed interannual variability. Until the 1970s, the MMM TCO gradually increases in the tropics (20S-20N), driven by the increase in the tropospheric columns, and in the NH mid-latitudes (35N-60N) where the tropospheric and stratospheric columns both increase (figure 2). Between the 1970s and the late 1990s, stratospheric ozone depletion leads to large TCO reductions in all regions and completely dominates the October TCO changes at southern high latitudes (60S-90S). There is also considerable ozone depletion at northern high latitudes (60N-90N) in boreal spring (March) between 1980s to the late 1990s. In the tropics and the NH mid-latitudes, the tropospheric columns continuously increase, which results in the TCO not dropping to below PI values. From the late 1990s, TCO starts to increase in all regions; this is largely driven by the change in the stratospheric columns. In the NH mid-latitudes and the Arctic polar region, the stratospheric ozone recovery is faster than in the respective regions in the SH, and in the tropics. The continuous increase of the tropospheric columns contributes substantially to the long-term TCO changes in the tropics and in the NH mid-latitudes. The models are much more consistent in simulating changes in the tropospheric columns, and the large model spread in TCO is dominated by the spread in the stratospheric columns (not shown). The model spread in TCO before 1970s is mainly governed by interannual variations but becomes much larger since the 1970s which is dominated by inter-model differences in the stratospheric column changes in response to the ODS changes (see Section 3.2.1).

3.2 Attribution of total and partial ozone column changes

Figure 3 shows the changes in MMM TCO due to the individual forcings, as deviations from 1850-1900 values. The ODSs contribute to the continuous substantial TCO reductions since the 1970s in all regions, with a reduction of over 150 DU in the springtime SH polar region, up to 60 DU in the NH polar region, 20−35 DU in both mid-latitude regions, and ∼10 DU in the tropics in the year 2000. The ozone increase since the late 1990s is more evident in the SH mid- and high latitudes, consistent with Antarctic ozone recovery. The increase in NTCFs leads to a gradual increase in TCO in all regions but has the largest impact in the NH mid-latitudes and the tropics, increasing by up to 15 DU and 9 DU respectively in 2014 compared to the PI period. The impact of NTCFs on polar ozone changes is relatively small. The methane increase results in TCO increases in all regions, ranging from 7 DU in the tropics, 15 DU in both mid-latitude regions, and up to 30 DU in both polar regions by the end of the simulation period. The combined impact from NTCFs and methane outweighs the impact from ODS in the near-global TCO changes. The increase of N_2O results in a steady, relatively small decrease in the near-global TCO since the period of 1850-1900 which however emerges in the SH only since the 1970s. The overall effect of N_2O on TCO changes amounts to ∼2 DU in the tropics and up to ∼10 DU reductions in the polar regions. The increasing CO_2 generally leads to a modest net reduction in TCO at the end of 2014 compared to its PI levels in all regions. The most significant reduction in TCO due to CO_2 occurred in the tropics since the 1970s, where TCO gradually decreased to ∼5 DU below its PI value in 2014. Note that there are some TCO increases in the NH mid- and high latitudes until the 1970s before values are declining, but there is a large interannual variation, especially in the NH polar region. The results from GISS-E2-1-G are not included in the MMM TCO changes but are shown in the supplement (Figure S1).

In the following we discuss the contribution of stratospheric and tropospheric partial columns to TCOs and the inter-model differences due to each forcing.

3.2.1 ODS

Figure 4 shows that the stratospheric column changes dominate the changes in TCO in all regions due to ODS. The model spread in TCO (expressed as the mean absolute deviation of annual mean values) is larger than the multi-model mean signal. Two mod-

els (CESM2-WACCM and GFDL-ESM4) are in good agreement and are much closer to the mean model values than the other two models. UKESM1-0-LL significantly overestimates ozone depletion in all regions relative to the MMM, and MRI-ESM2-0 generally underestimates ozone depletion, especially in the SH. The models show mostly a zero or slight positive trend in TCO after 2000, due to stratospheric ozone no longer declining in most regions.

3.2.2 NTCFs

Due to growing emissions of NTCFs, increases in tropospheric ozone columns dominate the TCO increase in the tropics and the NH mid-latitudes (Figure 5). In the SH mid-latitudes, the increase in stratospheric columns and the tropospheric columns are comparable. There are also moderate increases in TCO in the NH polar region, but the increase is not significant due to the large model spread there. The NTCFs have little impact on TCO in the SH high latitudes. The four models are in better agreement in simulating the TCO changes in the tropics and mid-latitudes than in high latitudes. Unlike the other models, UKESM1-0-LL shows a decrease, instead of an increase, in TCO since the late 1990s in the SH mid- and high latitudes. MRI-ESM2-0 shows a much larger increase in TCO in the polar regions than in the other models however with large interannual variation.

3.2.3 Methane

Methane causes TCO to increase in the extra-tropics since the 1970s (Figure 6). This increase is largely due to increases in extra-tropical stratospheric ozone. We discuss possible causes for this behaviour in section 3.3.3. In the tropics, the methane increase leads to a modest increase in TCO with comparable contributions from the stratosphere and the troposphere. The increase in tropospheric ozone columns also contributes to TCO increases, as CH_4 is an ozone precursor; the tropospheric increase has a proportionally larger impact on TCO in the tropics. The impact of methane increase on TCO in the polar regions is almost exclusively through the increase in the stratospheric columns, and is associated with a larger interannual variability than in the extra-polar regions. The three models that provided the data for assessing the methane impact on ozone are in good agreement, but the model spread becomes larger in the later decades of the simulation period and is particularly large in the SH polar region after the 1970s, likely as-

sociated with the large model differences in simulating polar ozone depletion (Figure 4) .

3.2.4 N_2O

The overall effect on global TCO from N_2O is small and mostly negative throughout the simulation period. It is dominated by changes in the stratospheric contribution (Figure 7). Two models (MRI-ESM2-0 and UKESM1-0-LL) provide the necessary data for assessing the impact of N_2O on ozone. The models are in good agreement before the later part of the 20^{th} century in all regions, but their results diverge towards the end of the simulation period (2014) in the extra-polar regions. In the tropics, the model difference becomes larger in the 1980s, but becomes smaller again after the year 2020. In the NH mid-latitudes, the model difference maximizes after year 2000 with MRI-ESM2-0 dropping to $\sim$7 DU below the PI value and UKESM1-0-LL gaining $\sim$5 DU above the PI value. In the SH mid-latitudes, the models also diverge after the year 2000 but the values at the end of the simulation period are still both negative compared to the PI times. The two models are in better agreement in the polar regions. Overall, the interannual variation seems larger than the model difference.

3.2.5 CO_2

Likewise, the impact of CO_2 on TCO as simulated by the same two models (MRI-ESM2-0 and UKESM1-0-LL) (Table 2) is dominated by changes in the stratospheric ozone columns (Figure 8). Both models show a steady decrease in TCO since the 1970s in the tropics, likely as a result of the change in the stratospheric circulation due to the CO_2 increase since the PI times (e.g. Butchart, 2014). The slight increase in near-global mean TCO (mainly driven by the increase in the NH) from 1850 to the 1970s is likely due to stratospheric cooling that reduces stratospheric ozone loss (Stolarski & Waugh, 2015). The sharp decrease in the stratospheric ozone columns after the 1970s coincides with the high loading of ODS, which, however, seems to enhance the stratospheric ozone depletion in a cooler stratosphere (see Section 3.3.5). In the high latitudes, the patterns of TCO changes are similar to the changes in the corresponding mid-latitudes, both with a large year-to-year variation. The two models agree reasonably well in simulating the impact of CO_2 on TCO but the model difference becomes larger after the 1990s in both the NH mid-latitudes and the SH polar region.

3.3 Response of global ozone changes to forcing

The response of changes in annual and zonal mean ozone concentrations in response to changes due to ODSs, NTCFs, methane, N_2O, and CO_2 are assessed using linear regression (Eqn. 1) over the whole simulation period of 1850-2014 (except for assessing ozone changes due to ODS which covers 1950-2014). With the exception of the ODSs, which peak in the late 1990s, the evolution of all other forcings is monotonic (Figure 1). Due to the short lifetime and the non-linearity of ozone and aerosol precursors, we use the multi-model and global mean surface ozone mixing ratios changes between 1850 to 2014 in the histSST simulation to represent the evolution of NTCFs in the linear regression. As expected, surface ozone increases monotonically between 1850 and 2014. All regressed variables, i.e., the forcing data, are normalised to range between 0 and 1. The purpose of expressing the ozone changes in concentration units is to demonstrate more directly how the vertically resolved ozone changes contribute to the column changes. Equivalent plots showing the response of ozone changes in volume mixing ratio to each forcing are displayed in the supplement (Figure S2-S6).

3.3.1 Response to ODS changes

The halogenated ODSs have increased sharply since the 1950s, peaking before the year 2000 and then decreasing (Figure 1). The response of ozone to these ODS changes, expressed as the linear regression coefficient, A_0, are shown in Figure 9 for the four models (CESM2-WACCM, GFDL-ESM4, MRI-ESM2-0, and UKESM1-0-LL). All models show an overwhelmingly negative ozone response with the largest ozone reductions in the high latitudes. Among the four models, UKESM1-0-LL displays the strongest Antarctic and Arctic ozone depletion, whereas MRI-ESM2-0 shows the weakest polar ozone depletion. The small increases in ozone in the tropics and the NH in MRI-ESM2-0 are insignificant at the 95% confidence level. The intermodel difference in the response to ODSs drives the large diversity in TCO changes (Figure 4).

3.3.2 Response to NTCFs changes

The ozone response to the increase in NTCFs is expressed as the linear regression coefficient, A_0, in Figure 10. The response is broadly consistent among the four models, and the main feature is the substantial increase in tropospheric ozone concentrations,

especially in the NH. All models show some increases in stratospheric ozone, although in CESM2-WACCM and GFDL-ESM4 such an increase is largely insignificant. The significant ozone increase in the lower to middle stratosphere in UKESM1-0-LL and MRI-ESM2-0 is likely due to these models' reduction in lower-stratospheric NO_y (not shown) that causes ozone to increase; this overestimation of stratospheric ozone changes will lead to a small overestimation in TCO in the MMM TCO. The UKESM1-0-LL also shows a significant ozone reduction in the SH lower stratosphere. The cause of this feature is unclear. We do not have sufficient diagnostics to ascertain if this is due to ozone-induced dynamical changes in that model.

3.3.3 Response to methane changes

Methane impacts ozone via a few positive feedback mechanisms. Methane is an ozone precursor which promotes ozone chemical production in the troposphere in the presence of NO_x. Through its reaction with OH, methane reduces the amount of HO_x-induced ozone loss in the stratosphere. It also reacts with free chlorine atoms (Cl), which are dominant ozone destructing compounds in the stratosphere, reducing ozone loss.

Three models (MRI-ESM2-0, GFDL-ESM4, and UKESM1-0-LL) have performed the methane perturbation simulation (histSST-piCH4). A linear regression function was constructed to assess the sensitivity of ozone to methane changes between 1850 and 2014 (Figure 11). It shows that the response of ozone to the methane increase is positive in the troposphere in all models. In the stratosphere, the ozone response is also largely positive primarily through its reaction with free Cl to produce HCl which reduces the amount of reactive chlorine available to destroy ozone. This effect is particularly strong in the lower stratosphere polar regions where Cl-induced ozone depletion is most abundant and the strongest. Reader et al. (2013) calculated a reduction of 15-35% in reactive chlorine throughout the stratosphere due to methane increase from the PI to present-day under high chlorine load conditions. There is a reduction in ozone in the upper stratosphere and mesosphere where the dissociation of H_2O becomes more important, which promotes ozone reduction through increased HO_x there (Morgenstern et al., 2018). This negative effect of methane on mesospheric ozone is simulated by all four models (figure S4). There are also some reductions of ozone in the tropical middle stratosphere, most pronounced in MRI-ESM2-0 and GFDL-ESM4, which could be caused by the HO_x-induced ozone loss through the dissociation of water vapour that outweighs the other processes.

Although the models agree well on the largely positive feedback from the methane increase, there are some inter-model differences, in particular the stronger ozone increases in the polar regions in MRI-ESM2-0 and UKESM1-0-LL than that in GFDL-ESM4. There are small decreases in ozone in the tropical lower stratosphere in both MRI-ESM2-0 and GFDL-ESM4, but not in UKESM1-0-LL.

3.3.4 Response to N_2O changes

Two models (MRI-ESM2-0 and UKESM1-0-LL) have performed N_2O perturbation simulations (histSST-piN2O). The ozone change in response to the N_2O increase, shown in Figure 12, is characterised by the reduction in ozone in the middle and upper stratosphere and an increase in ozone in the upper troposphere and lower stratosphere (UTLS) in both models. The increase in N_2O increases the availability of odd-nitrogen causing ozone destruction in the stratosphere. The increase in ozone concentrations in the UTLS region is likely due to a "self-healing" process as reduced overhead ozone columns allow more ultraviolet light to penetrate to lower levels, producing more ozone there. In the presence of ODSs, the increasing N_2O has a positive impact on ozone changes in the stratosphere, mainly due to the reaction between NO_2 and chlorine monoxide (ClO) forming $ClONO_2$ which reduces the efficacy of chlorine-catalysed ozone depletion. The reduction in ozone in the SH polar region is likely due to the self-healing process mentioned above.

The ozone responses to increasing N_2O over this historical period are consistent in the two models, however with a stronger ozone reduction occurring in the NH high latitudes in MRI-ESM2-0 and in the SH high latitudes in UKESM1-0-LL, respectively. Although the overall impact on TCO from increasing N_2O is rather small (Fig 7) over this historical period, the negative impact from increasing N_2O on ozone could become more significant with halogenated ODSs declining in the future (Ravishankara et al., 2009; Revell et al., 2012).

3.3.5 Response to CO_2 changes

Ozone changes in response to the CO_2 increase are assessed in two models (MRI-ESM2-0 and UKESM1-0-LL), and are calculated by subtracting all other single-forcing responses from the all-forcing simulation (Table 2). Again, a linear regression function

is applied to regress ozone changes on the normalised changes in CO_2. The resulting linear regression coefficient (Figure 13) shows that, in both models, the increase in CO_2 leads to a significant ozone increase in the middle and upper stratosphere and a decrease in the UTLS region. This is consistent with previous findings that increasing CO_2 can modify ozone concentrations through chemical and dynamical changes in the stratosphere which we elaborate on below: The slowdown of ozone destruction due to cooling caused by the CO_2 increase (e.g. Haigh & Pyle, 1979; Portmann et al., 2012) will lead to ozone increases. In the SH polar region, however, the major reduction in ozone concentrations in the lower stratosphere is due to stratospheric cooling which promotes the formation of polar stratospheric cloud, causing ozone depletion. The rise of the tropopause due to the speedup of the Brewer-Dobson circulation (BDC; Oberländer-Hayn et al., 2016) modifies the distribution of ozone leading to ozone reductions in the lower stratosphere and the upper troposphere. The speedup of the BDC also leads to faster poleward transport of stratospheric ozone that results in decreased ozone in the tropical lower stratosphere but increased ozone in the extra-tropics (Shepherd, 2008; Li et al., 2009). The ozone loss in the troposphere is also linked to enhanced photochemical destruction in a wetter and warmer climate due to CO_2 increase (e.g. Johnson et al., 1999).

3.4 Attribution of recent vertically resolved regional ozone trends

We assess regionally averaged multi-model mean vertically resolved ozone trends in the "histSST" simulation and the attribution of those trends in ozone to ODS, NTCFs, and GHGs for both the ozone depletion period (1979-1999) and the ozone recovery period (2000-2014). The impacts of ODS and NTCFs can be assessed directly from the respective perturbation simulations. The impact of the combined GHGs on ozone was derived as a residual from the perturbation simulations of ODSs and NTCFs (table 2) for a more direct comparison with the CCMI-1 models (WMO, 2018). In addition, we also show separately the impacts of methane and the combined CO_2 and N_2O (namely "LL-GHGs") on ozone trends from the available three model results, as only two models provided the perturbations for assessing the impact of CO_2 and N_2O separately. We focus on analysing the ozone changes in three regions including the NH mid-latitudes (60N-35N), the tropics (20N-20S), and the SH mid-latitudes (35S-60S). The trends and their contributions are shown separately for the stratosphere and the troposphere.

3.4.1 Stratosphere 1979-1999

Figure 14 shows the percentage change in vertically resolved ozone concentrations and the contribution of each forcing to the overall ozone trend in the stratosphere for the ozone depletion period (1979-1999). The resulting ozone trend is statistically significant negative throughout the stratosphere, predominantly driven by ODS increases. In the upper stratosphere, a negative trend of ∼4-6% per decade occurs in the mid-latitudes and ∼ −2-4% per decade in the tropics, caused by halogen-induced ozone depletion. In the middle stratosphere (30-10 hPa), the trend becomes smaller. The most pronounced ozone reduction (up to ∼ 8% per decade) is in the SH mid-latitudes which is impacted by Antarctic ozone depletion. Arctic ozone depletion also results in a ∼3-4% per decade decrease of ozone in the NH mid-latitude lower stratosphere. In the tropical lower stratosphere, the negative trend in ozone becomes insignificant due to large uncertainty (a combination of model and statistical uncertainties) in this region.

Contributions from other forcing agents to the ozone trend are relatively small during this period. The NTCFs have no significant impact on stratospheric ozone. The combined GHGs (methane, CO_2, and N_2O) lead to a small but significant positive ozone trend in the extra-tropical upper stratosphere, a negative trend in the middle stratosphere in the NH mid-latitudes, and a negative trend between the middle and upper tropical stratosphere. Among the individual GHGs, the increase in methane generally leads to a positive trend in ozone in the stratosphere whereas the impact from the combined CO_2 and N_2O leads to a small negative trend in ozone. Note that the impacts from methane and LLGHGs are based on three models. In the lower stratosphere, the ozone trend is associated with a larger uncertainty than in the upper and middle stratosphere, especially in the tropics where the ozone trend is insignificant at the 95% confidence level.

3.4.2 Stratosphere 2000-2014

Over the 2000-2014 period, the ozone trends, although largely positive, are mostly insignificant, except in the upper stratosphere where the ozone concentration shows a significant increase of up to 3% per decade (Figure 14). The contrast in stratospheric trends between the two periods is the consequence of the declining ODS concentrations since the late 1990s. During this period (2000-2014), ODSs are in a slow decline. Ozone

trends due to ODSs are comparable to the impacts of the combined GHGs; both contribute to a positive trend in the upper stratosphere.

The impact of methane on the ozone trend is mainly negative in the upper stratosphere, emphasising that its impact on stratospheric ozone depends on the background ODS levels. As ODS concentrations decline, the positive impact of methane on stratospheric ozone becomes smaller. In the lower stratosphere, the methane increase leads to ozone increases in the NH mid-latitudes and in the tropics, through chemical ozone production, also shown in the period 1979-1999.

The increase of LLGHGs (CO_2 and N_2O) leads to positive ozone trends in the upper stratosphere as the result of the slowdown of ozone chemical destruction in a cooler stratosphere caused by the CO_2 increase. As ODS concentrations decline, CO_2 plays an increasingly important role in driving stratospheric ozone trends. It shows that the increasing LLGHGs lead to a positive ozone trend in the upper stratosphere due to continuous cooling. The negative contribution from the LLGHGs to the ozone trend in the lower stratosphere is the consequence of the dynamical change due to CO_2 increase The increases in N_2O and CO_2 have a conflicting influence on ozone changes, but the influence from CO_2 outweighs that from N_2O. Although CO_2 dominates the impact from LLGHGs, N_2O could also have a significant impact on the future trend in stratospheric ozone. Increasing N_2O generally causes stratospheric ozone loss by nitrogen-induced ozone destruction, but such a negative feedback is dampened in the presence of ODSs due to the formation of $ClONO_2$ which reduces both NO_x- and Cl-induced ozone depletion. Therefore, the impact on stratospheric ozone from increasing N_2O is expected to be more pronounced in the future when ODSs decline. However, we cannot diagnose a significant trend here due to a large discrepancy existing between the two available model's estimation of the N_2O impact after the 1990s (Figure 7).

Overall, the response of stratospheric ozone trends to changes in ODSs and GHGs in these models is consistent with those found previously in CCMI-1 models (WMO, 2018). A common feature is the large variability in the modelled lower stratospheric ozone trends. In the CMIP6 models included in this study, the largely insignificant lower stratospheric ozone trends over the period of 2000-2014 also reflect the relatively short period and the resulting small changes in forcing. However, the trend reversal in stratospheric ozone due to ODS reductions is clearly simulated in these CMIP6 models. The limited number of

models also increases the uncertainty in estimating the ozone trends over this short period.

3.4.3 Troposphere

Over the 1979-1999 period, Figure 15 indicates that there is an insignificant negative ozone trend of $\sim$ 3%/decade in the NH mid-latitudes upper troposphere and a significant negative trend of $\sim$8%/decade in the SH mid-latitudes upper troposphere. These negative trends in the mid-latitudes become positive in the free and lower troposphere. In the tropics, a significant positive trend of $\sim$ 5% per decade occurs throughout the troposphere over this period. Over the 2000-2014 period, the ozone trend in the extra-tropical upper troposphere has shifted from negative to small though insignificant positive. In the tropical and extratropical free and lower troposphere, there are no significant changes in ozone trend in these regions compared to the previous period.

Although the increase of ozone precursors (i.e., NTCFs) largely dominates the ozone trend in the free and lower troposphere, the stratospheric ozone change due to ODS has a large significant impact on the extra-tropical ozone trend in the upper troposphere, especially in the SH over the period of 1979-1999. This impact is much reduced over the period 2000-2014, emphasising the impact of stratospheric changes on tropospheric ozone.

The impact of GHGs on the tropospheric ozone trend is a combined effect from the changes in methane and the LLGHGs. The increase in methane contributes positively ($\sim$2-3%/decade) throughout the troposphere during the 1979-1999 period, but this contribution is much reduced in the free and lower troposphere over the period 2000-2014; this is more evident in the SH mid-latitudes where the ozone trend has changed from positive to negative due to methane which may be due to the reduced positive feedback from increasing methane to ozone with the lower ODS loading during this period. The impact from the LLGHGs (i.e., a combination of CO_2 and N_2O) on tropospheric ozone is predominantly negative with generally a larger impact in the upper than in the lower troposphere, especially in the extra-tropics. The changes in upper tropospheric ozone due to LLGHGs is associated with a large uncertainty reflecting dynamical variability. A warmer troposphere due to the CO_2 increase leads to the increase in water vapour which promotes ozone chemical destruction. (e.g. Stevenson et al., 2006). Overall, the combined change in GHGs leads to a small and mostly positive ozone trend of less than $\sim$2-

559 3% per decade in the period 1979-1999 and a close to zero trend in the period 2000-2014
560 which is largely due to the decreasing impact of methane on lower tropospheric ozone.

561 3.5 Impact of stratospheric changes on tropospheric ozone

562 *3.5.1 Mean stratospheric age of air*

563 A change in stratospheric circulation affects tropospheric ozone through stratosphere-
564 troposphere exchange (STE); it is often characterized in terms of stratospheric age of
565 air (AoA). Here we quantify the change in AoA and its attribution to individual forc-
566 ings in two models (UKESM1-0-LL and MRI-ESM2-0) that have provided the diagnos-
567 tics of the mean AoA. Figure 16 shows the AoA changes averaged over 1-70 hPa from
568 1870 to 2014 in the "all forcings" histSST simulation and the impact of forcing based
569 on their perturbations simulations from the two available models. In both models, the
570 AoA decreases substantially after the 1960s, reaching a reduction of 0.7 years in MRI-
571 ESM2-0 and 0.8 years in UKESM1-0-LL in the late 1990s before leveling off, albeit with
572 considerable interannual variability. The reduction in the AoA in both models reflects
573 an acceleration of stratospheric overturning, i.e., the Brewer-Dobson circulation (BDC).
574 The reductions in AoA in both models are clearly driven by ODS and CO_2 increases.
575 In UKESM1-0-LL, the impact of ODS and CO_2 on AoA are similar in magnitude; each
576 contributes ∼0.5-0.6 years to the AoA decrease over the ozone depletion period(Polvani
577 et al., 2019). The impacts from other forcings (methane, N_2O, and NTCFs) on AoA are
578 small in UMESM1-0-LL. In MRI-ESM2-0, the impact of ODS on AoA (∼0.2 years of re-
579 duction) is smaller than in UKESM1-0-LL, in agreement with the weak ozone depletion
580 exhibited by this model. In this model, the diagnostic of the AoA change due to NTCFs
581 is not available, hence we show the combined CO_2 and NTCFs effect which is ∼0.4 years
582 in AoA reduction. The impacts from methane and N_2O on AoA are also small in MRI-
583 ESM2-0.

584 *3.5.2 Stratosphere-troposphere exchange*

585 We now examine the impact of anthropogenic forcings on STE in the models. Due
586 to a lack of available diagnostics to directly evaluate STE, we use an indirect approach,
587 i.e. we calculate the residual of the ozone flux in the troposphere assuming it is balanced
588 by net photochemical production and dry deposition of ozone (Griffiths et al., 2021). Fig-

ure 17 shows the evolution of STE anomalies in histSST and due to the respective forcings relative to their PI values in four models. All models show various degrees of decreases in STE since the 1950s, with the largest decrease occurring in UKESM1-0-LL reaching to the lowest point in around 2000 (~ -370 Tg(O_3)/year), followed by CESM2-WACCM (-150 Tg(O_3)/year), GFDL-ESM4 (-50 Tg(O_3)/year), and MRI-ESM2-0 (-25 Tg(O_3)/year). The impact of ODS increases lead to large STE decreases in all models except in MRI-ESM2-0. Roughly half of the net decreases in STE are due to ODSs in UKESM1-0-LL and CESM2-WACCM. In GFDL-ESM4, there is a reduction of $\sim$60 Tg(O_3)/year due to ODSs, which is larger than the STE reduction due to all forcings combined. The substantial reduction in STE due to stratospheric ozone depletion is consistent with the finding by Hegglin (2009).

Another significant driver for reductions in STE is NTCFs (Figure 17), whereby the increase in NTCFs produces a decrease in STE in three of the four models. This suggest that tropospheric ozone increases reduce the net downward transport of ozone from the stratosphere. By contrast, the methane increase causes a consistent increase in STE among the three models which performed methane perturbation simulations. The increase is a consequence of the stratospheric ozone increases caused by growing methane concentrations.

Of the two models in which the impact of CO_2 can be assessed separately, the increase in CO_2 leads to a reduction in STE in UKESM1-0-LL but such an impact is less clear in MRI-ESM2-0. The combined impact from CO_2 and N_2O also shows a reduction in STE in GFDL-ESM4. As N_2O changes do not show any clear impact on STE in UKESM1-0-LL and MRI-ESM2-0, we assume that its impact on STE is also minor. Therefore the reduction in STE due to combined NO_2 and CO_2 in GFDL-ESM4 is mostly caused by the increase in CO_2. This reduction in STE due to CO_2 increase is likely the result of the decreased ozone in the lower stratosphere (cf. Figure 13).

3.5.3 Impact on surface ozone

Finally, we examine the impact of different forcings on global-mean surface ozone. Figure 18 shows the evolution of mean surface ozone anomalies since 1850 in histSST and the anomalies due to individual forcings. As expected, the monotonic increase in surface ozone since 1850 is largely driven by the increase of NTCFs, followed by the increase

in methane. The change in ODS loading leads to continuous surface ozone reduction since the 1970s and reached the maximum reduction of ∼3 ppbv in 2000 in all models except in MRI-ESM2-0. This is the result of reduced downward transport of stratospheric ozone (cf. Section 3.5.2). The increase of N_2O has no discernible impact on global-mean surface ozone from the two available model results. CO_2 increases lead to a continuous decrease in surface ozone with a reduction of $\sim$ 3 ppbv in all models, which is consistent with the negative feedback from CO_2 to tropospheric ozone. Note that in GFDL-ESM4, this impact also includes that from N_2O, although small, as there is no separate fixed N_2O simulation available from this model. Here, the results corroborate with the finding by Tarasick et al. (2019) that the stratospheric changes not only impact significantly on ozone in the upper and free troposphere, they also significantly impact the lower tropospheric ozone.

4 Summary and conclusions

We have assessed the response of historical ozone changes to the anthropogenic forcings of ODSs, NTCFs, methane, N_2O, and CO_2 using the CMIP6 AerChemMIP perturbation simulations, and have quantified the contributions of each individual forcing to the changes in total, stratospheric, and tropospheric ozone columns. Consistent with previous studies, ODS-induced ozone depletion dominates the stratospheric ozone changes from the 1970s until the late 1990s, followed by a stable or a slightly upward trend between 2000 and 2014 when the ODS forcing declines. Methane increases, during periods of high Cl loading, significantly contribute to stratospheric column ozone increase. N_2O increases impact TCO by reducing the stratospheric ozone columns, but the overall effect is relatively small. CO_2 increases lead to an increase in the stratospheric ozone columns in the NH and the tropics before the 1970s, then followed by a decrease in the stratospheric ozone column coinciding with the ODS increase. We find that increases in the short-lived ozone precursors and methane lead to a substantial increase in tropospheric ozone since the 1950s that is increasingly important to the total column ozone. All models agree qualitatively on the response of ozone changes to the individual forcings but differ substantially in their simulations of ODS-induced ozone depletion - the largest source of inter-model differences. There is also a large interannual variation in stratospheric ozone columns due to changes in N_2O and CO_2.

We have examined the contributions of these forcings to recent regional ozone trends (NH and SH mid-latitudes and the tropics) for the periods 1979-1999 and 2000-2014. The results confirm that ODSs are the dominant forcing for the significant negative stratospheric ozone trends over the 1979-1999 period. Methane increases contribute to the stratospheric ozone increase in all regions, whereas the combined N_2O and CO_2 forcing drives an ozone decrease. Consequently, the combined GHGs produce a small positive contribution to the upper stratospheric ozone trend. The post-2000 stratospheric ozone change shows a weak positive trend driven by the reduction in ODS since the late 1990s. The trend is only statistically significant at the 95% confidence level in the upper stratosphere, if both model and statistical uncertainties are accounted for. Due to the ODS declines, the impact of methane on stratospheric ozone has also reduced. The combined CO_2 and N_2O impacts lead to a positive ozone trend in the upper stratosphere, in response to the declining ODS during this period. However, the short period of declining ODS loading (2000-2014) available for this analysis and small changes in forcing lead to a larger uncertainty in modelled ozone trends in this period, especially in the lower stratosphere where ozone changes are typically associated with large dynamical variability.

The ozone trends in the troposphere are predominantly positive throughout the periods 1979-1999 and 2000-2014, mainly driven by increases in short-lived ozone precursors and methane. However, stratospheric ozone depletion causes a significant negative ozone trend in the upper troposphere extra-tropics for 1979-1999. There is a trend reversal between 2000 and 2014 which coincides with the decline in ODSs. The impact of GHGs on the tropospheric ozone trend is relatively small and is a balance between a positive effect from methane increases and a negative effect from the LLGHGs (CO_2 and N_2O) increases. The mean AoA shows reductions of 0.7-0.8 years compared to PI conditions in two models, reflecting an acceleration of stratospheric overturning since the 1950s, mainly due to increases in ODS and CO_2. We have also derived STE of ozone from the models' tropospheric ozone budget, assuming that the production and loss terms are in balance: The changes in ODS, CO_2, methane, and the ozone precursors are responsible for trends in the STE. The reduction in stratospheric ozone combined with the acceleration of the BDC leads to a reduced residual of the stratospheric ozone in the troposphere, while the increase in tropospheric ozone production due to the short-lived ozone precursors reduces STE. Methane increases cause increases in stratospheric ozone, which promotes downward transport of ozone leading to an increased STE. Whilst the major

contribution to the surface ozone increase is due to ozone precursors, the increase in ODSs and in CO_2 nevertheless each leads to a 2-4 ppbv reduction in global mean surface ozone.

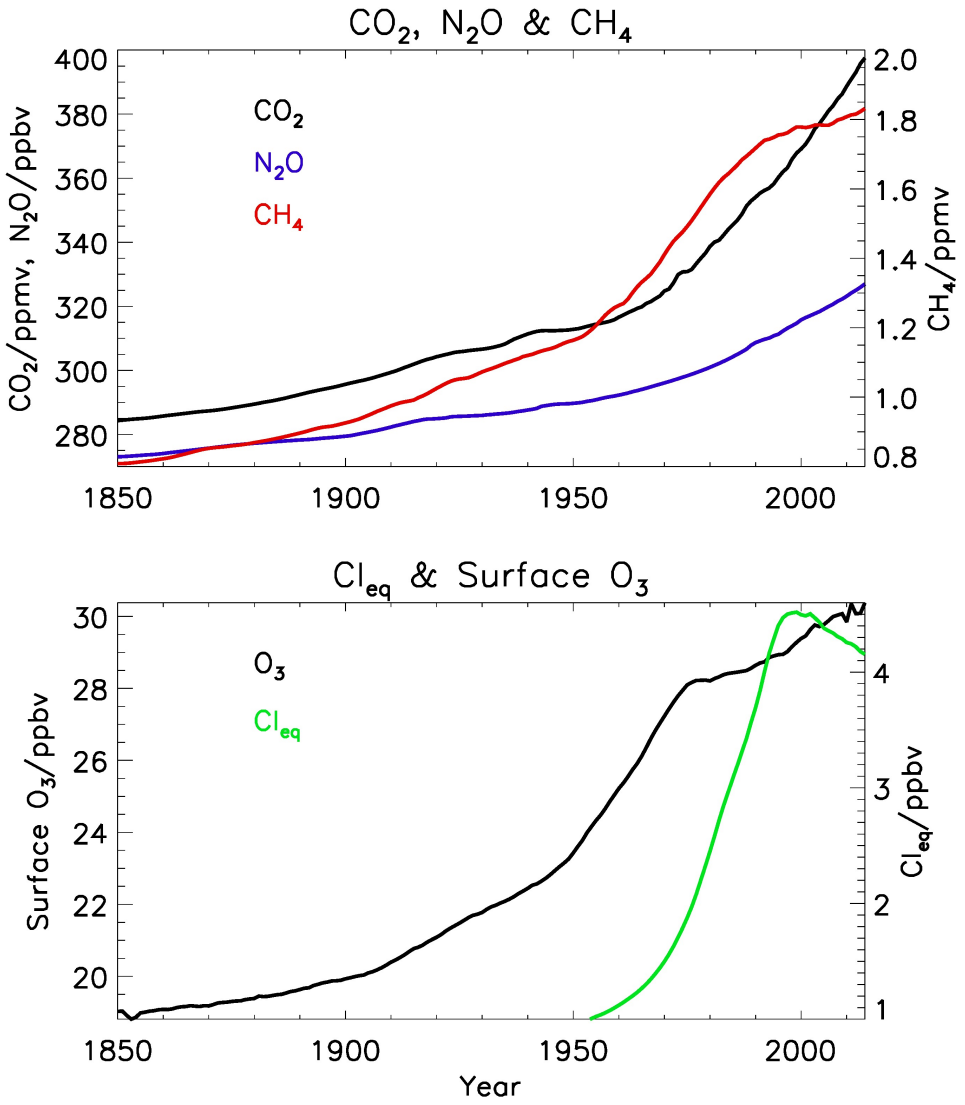

Figure 1. Annual-mean CO_2, N_2O, CH_4, equivalent chlorine (Cl_{eq}), and global- and multi-model mean surface ozone between 1850 and 2014 used as regressors in this study. Apart from surface ozone, the data are taken or derived from the CMIP6 "historical" scenario (Meinshausen et al., 2017). Surface ozone represents the evolution of ozone precursors.

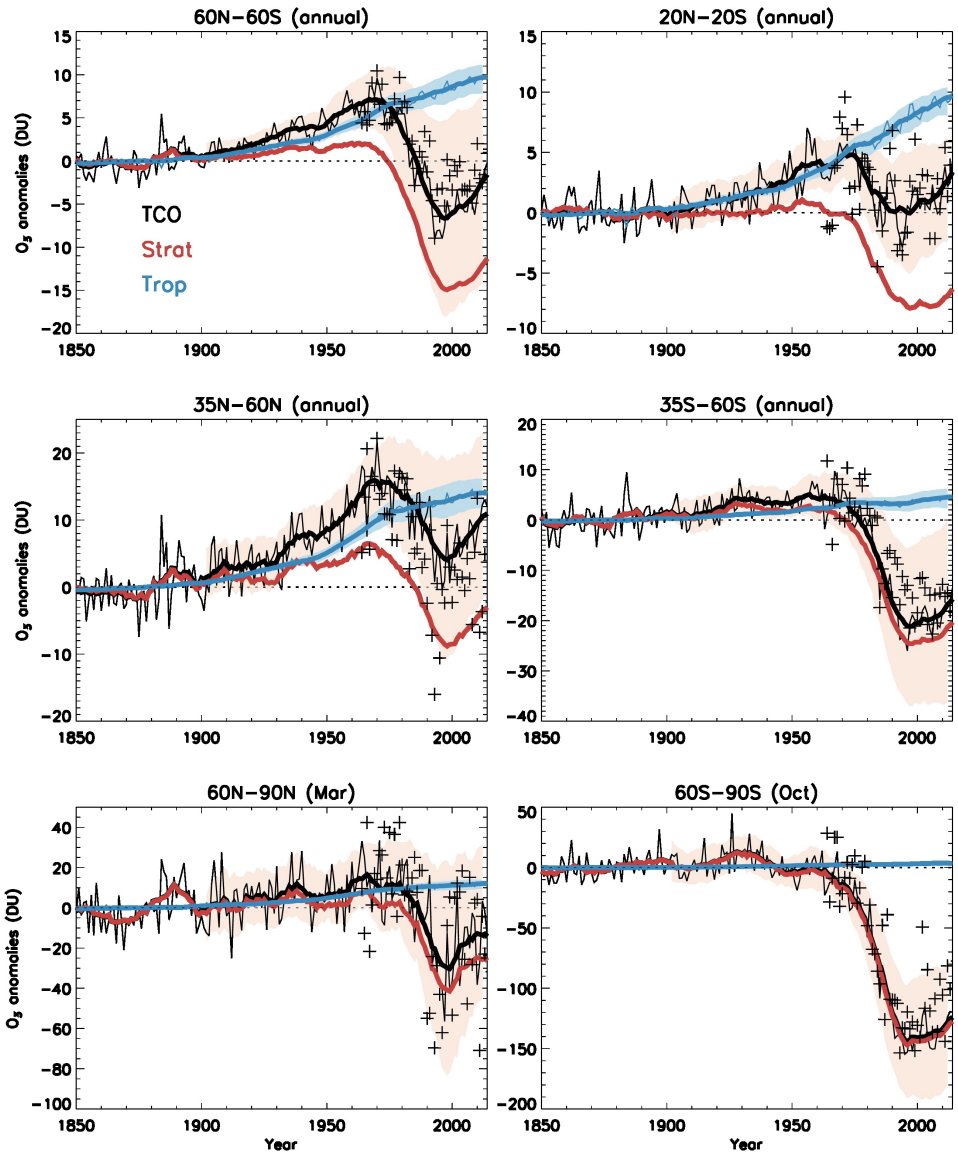

Figure 2. Multi-model mean (MMM) deviations of total, stratospheric, and tropospheric column ozone from the mean values of 1850-1900 regionally averaged for six regions. (colored thick lines) Smoothed MMM deviations using a 20-year boxcar filter. (grey thin lines) Annually resolved unfiltered MMM TCO. (haded areas) Annually resolved model deviations (expressed as the mean absolute deviations (MAD)) for TCO and tropospheric columns (the MAD for the stratospheric columns are not shown here but is similar to that of the TCO). The tropopause is defined using the WMO lapse rate definition in each model. Four models (CESM2-WACCM, MRI-ESM2-0, UKESM1-0-LL, and GFDL-ESM4) are included in the ensemble mean. Observations ("+") are from the World Ozone and UV Data Center's ground-based climatology (Fioletov et al., 1999) (https://woudc.org/archive/Projects-Campaigns/ZonalMeans/).

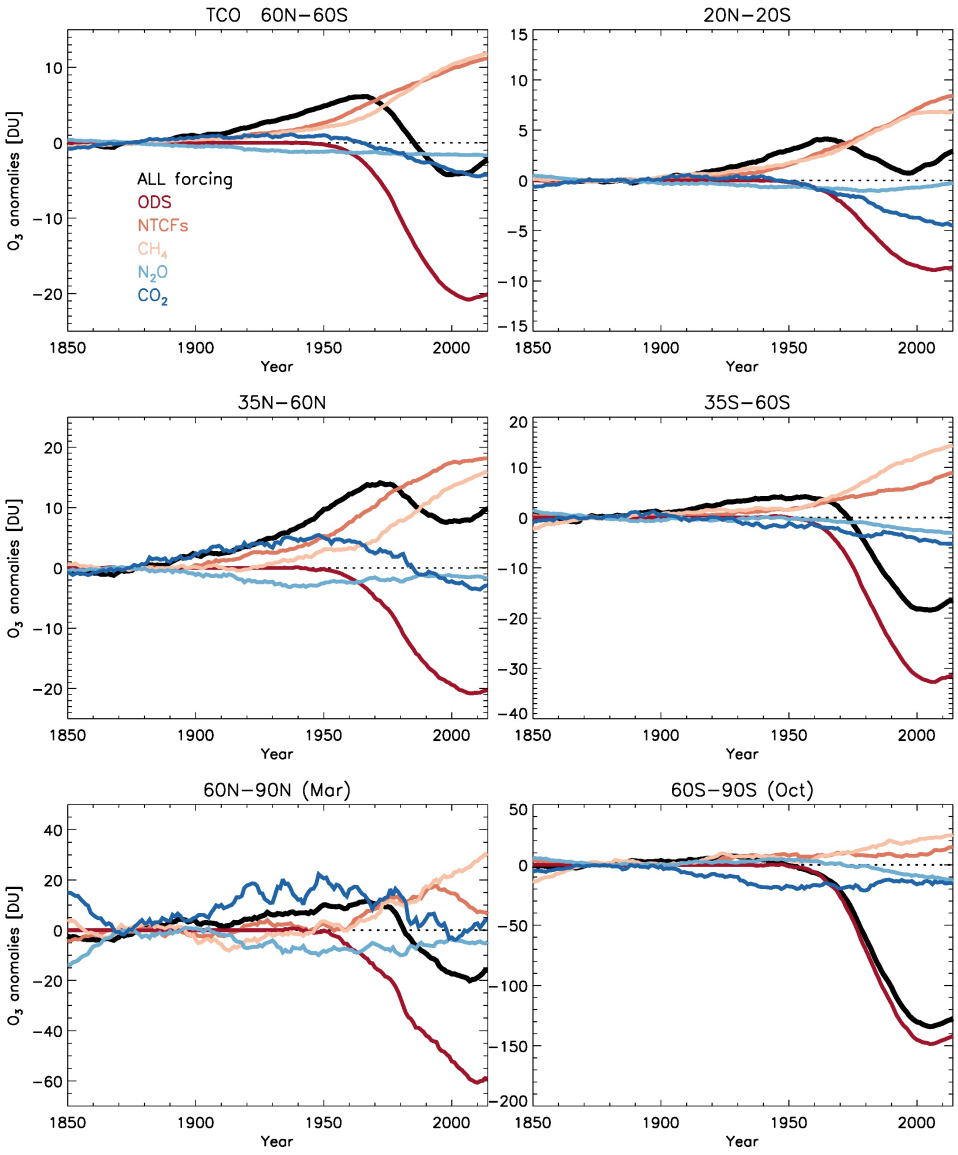

Figure 3. Multi-model mean TCO differences due to changes in individual forcings from 1850 to 2014. Displayed are annual mean data (for the near-global, tropics, and mid-latitude regions) and monthly mean March and October data (for the polar regions) smoothed using a 20-year boxcar filter. Black: all forcings. Red: ODSs. Dark orange: NTCFs. Light orange: CH_4. Light blue: N_2O. Dark blue: CO_2.

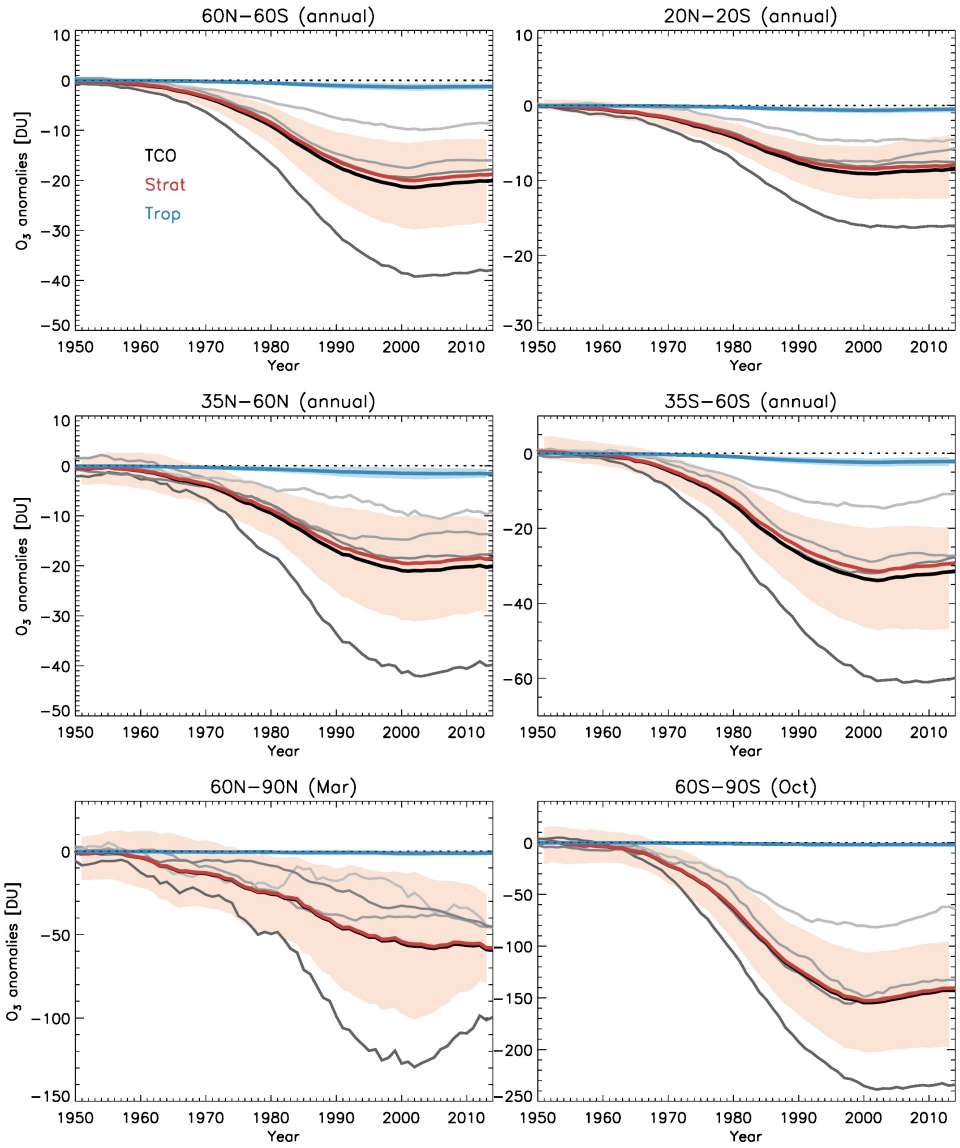

Figure 4. Changes in TCO and in the stratospheric and tropospheric ozone columns due to changes in ODSs from 1950 to 2014. Multi-model mean of TCO (black), stratospheric columns (red), and tropospheric columns (blue) are shown in thick lines, and are smoothed using a 20-year boxcar filter. Shaded areas are the mean absolute deviations (MAD) of unfiltered annual mean values in MMM TCO. Grey lines are TCO (smoothed with a 20-year boxcar filter) from the individual models; in the order of light to dark grey for MRI-ESM2-0, CESM2-WACCM, GFDL-ESM4, and UKESM1-0-LL.

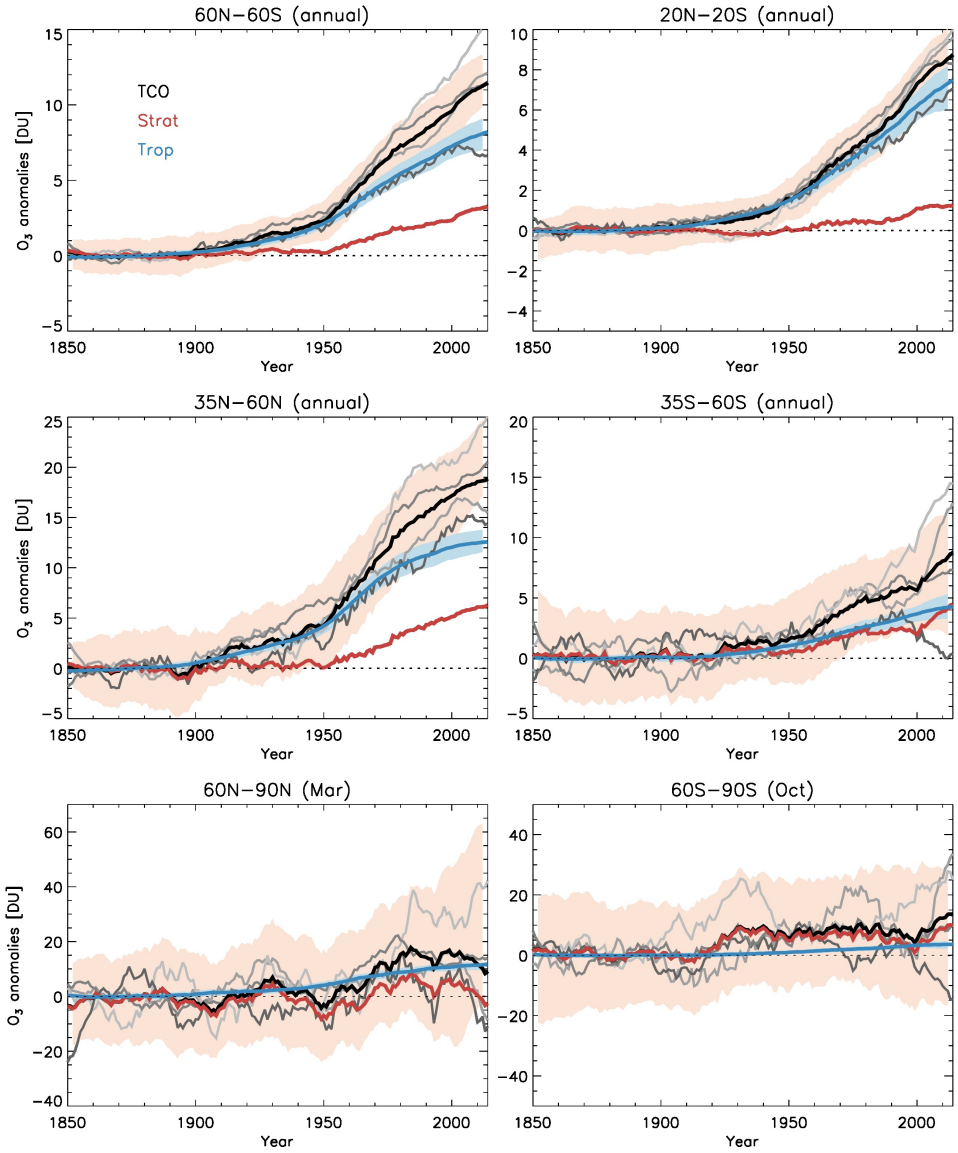

Figure 5. Same as Figure 4, but for NTCFs (1850-2014).

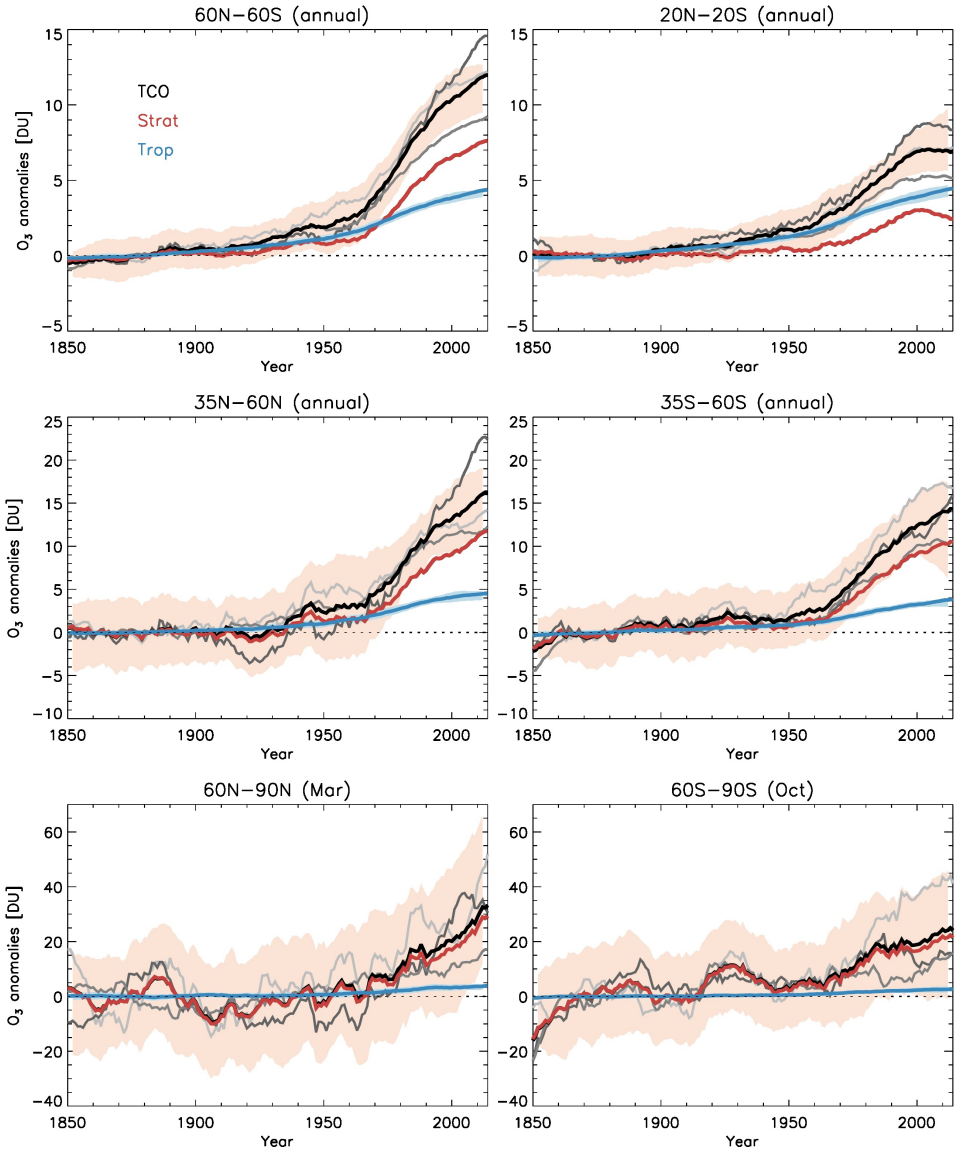

Figure 6. Same as Figure 4, but for methane (1850-2014). Results are from three models (MRI-ESM2-0, GFDL-ESM4, and UKESM-0-LL).

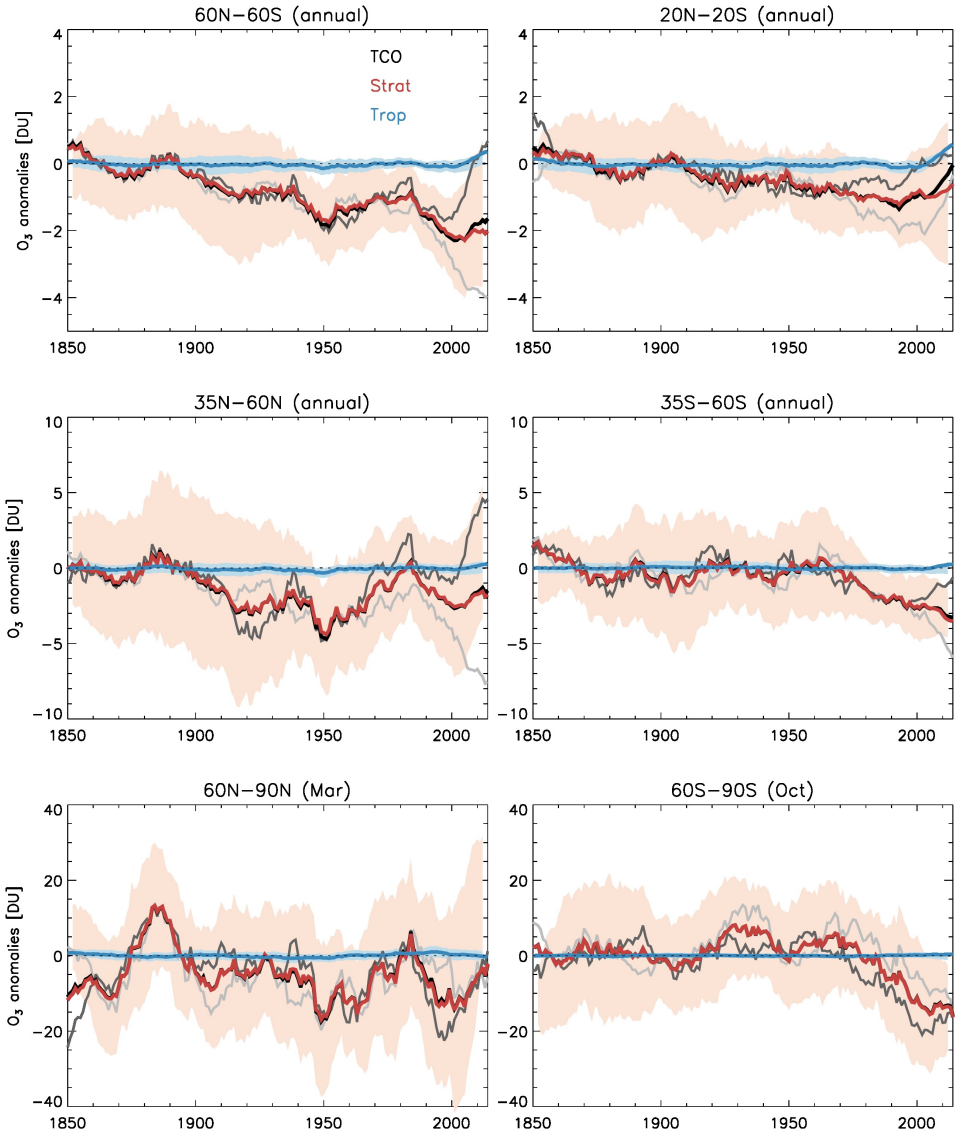

Figure 7. Same as Figure 4, but for N_2O (1850-2014). Results are from two models (MRI-ESM2-0 and UKESM1-0-LL).

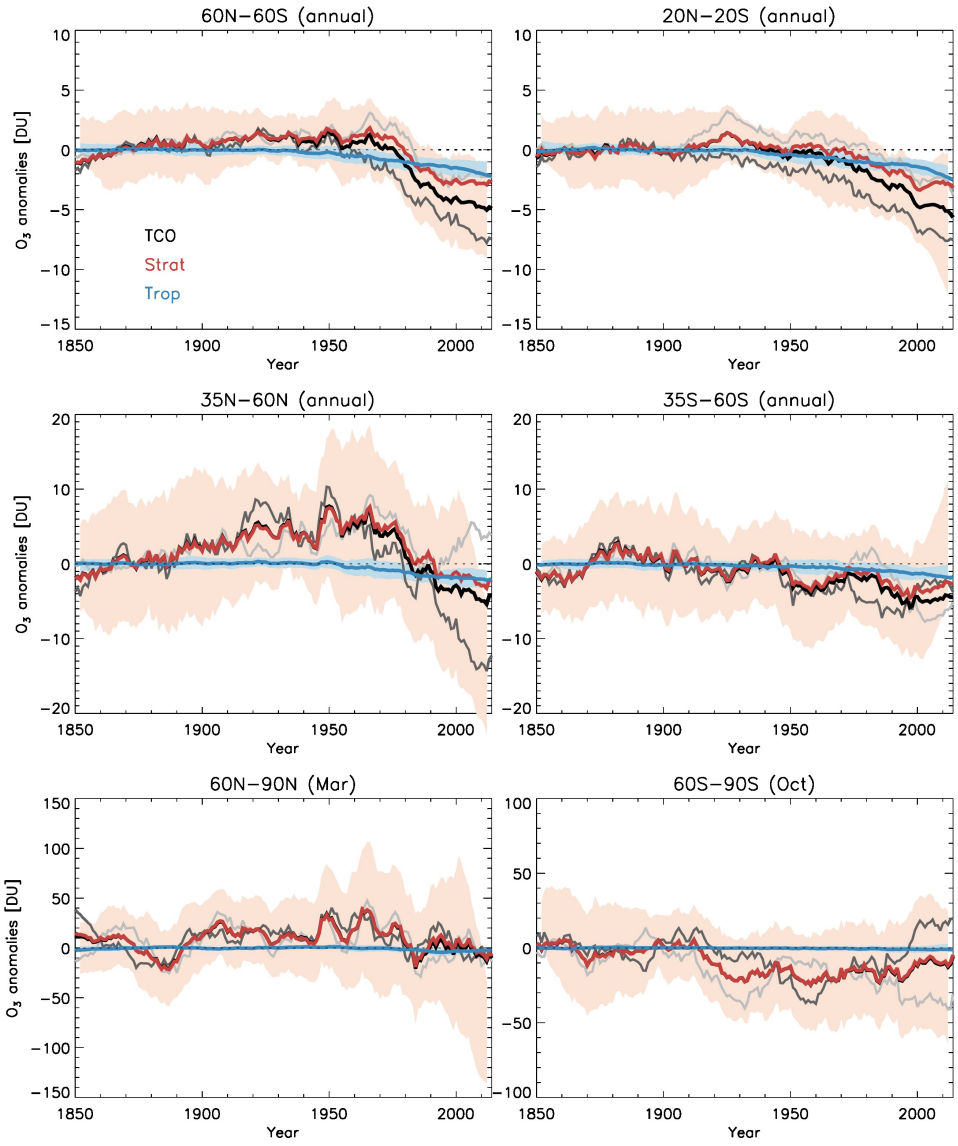

Figure 8. Same as Figure 4, but for CO_2 (1850-2014). Results are from two models (MRI-ESM2-0 and UKESM1-0-LL).

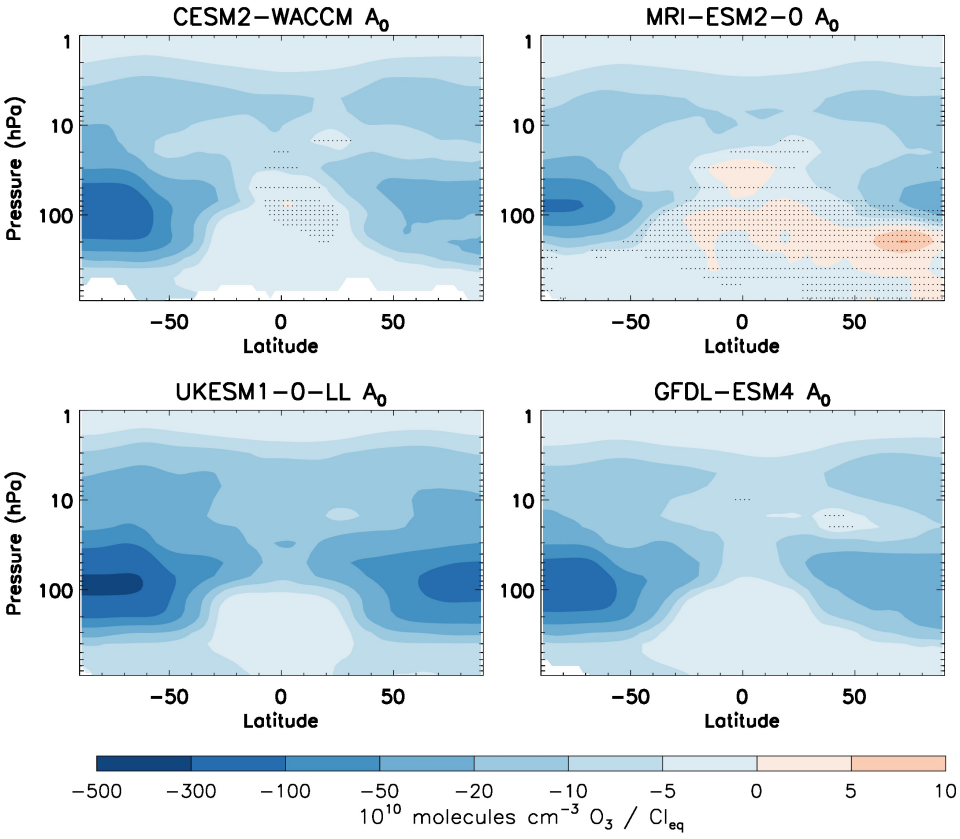

Figure 9. Ozone concentration changes (molecules cm^{-3}) in response to changes in Cl_{eq} (normalised to the range of 0 to 1) between 1850 and 2014. Stippled regions exhibit statistically insignificant responses at the 95% confidence level.

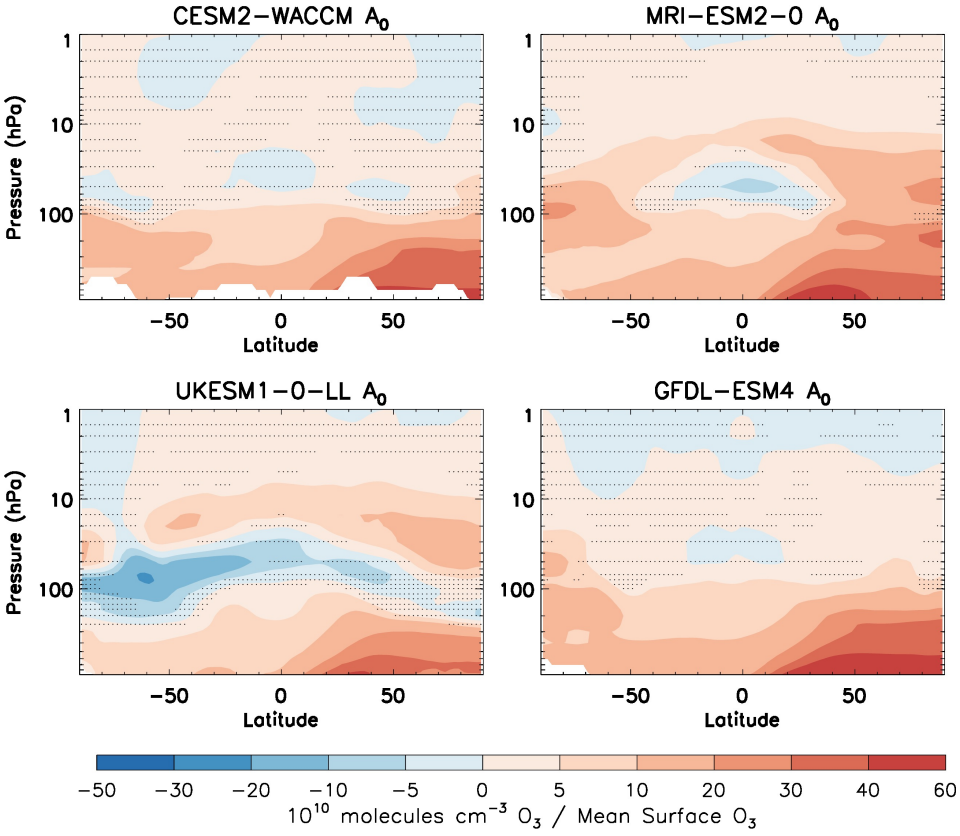

Figure 10. Ozone concentration changes (molecules cm^{-3}) in response to changes in ozone precursors (NTCFs) expressed as the mean surface ozone (normalised to the range of 0 to 1) in models. Stippled regions exhibit statistically insignificant responses at the 95% confidence level.

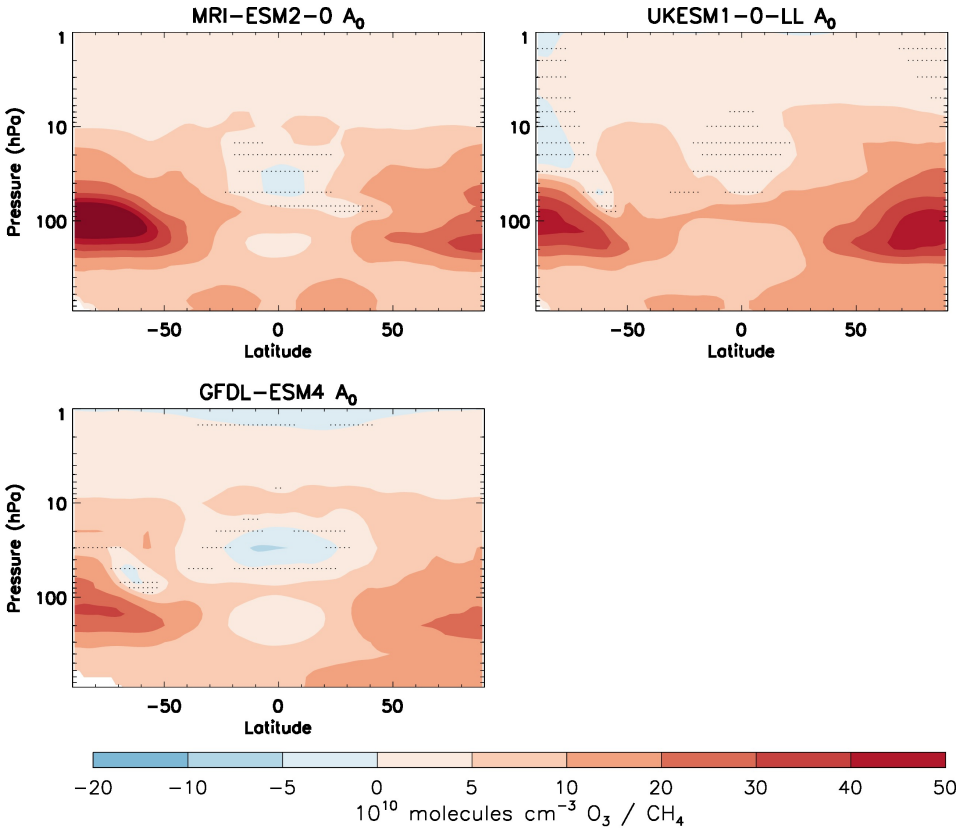

Figure 11. Ozone concentration changes (molecules cm^{-3}) in response to changes in methane (normalised to the range of 0 to 1) in models. Stippled regions exhibit statistically insignificant responses at the 95% confidence level.

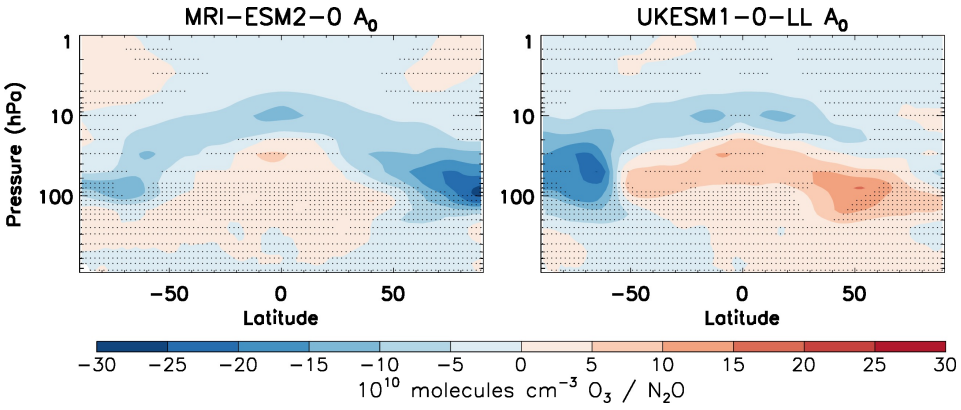

Figure 12. As Figure 11, but for N_2O.

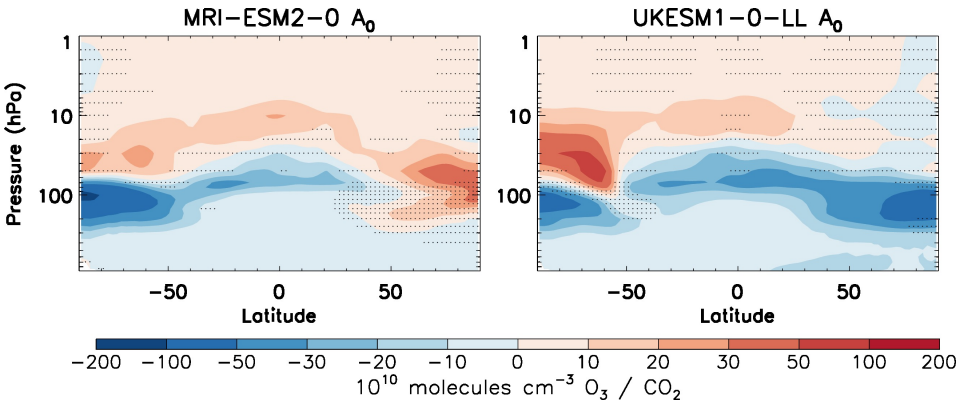

Figure 13. As Figure 11, but for CO_2.

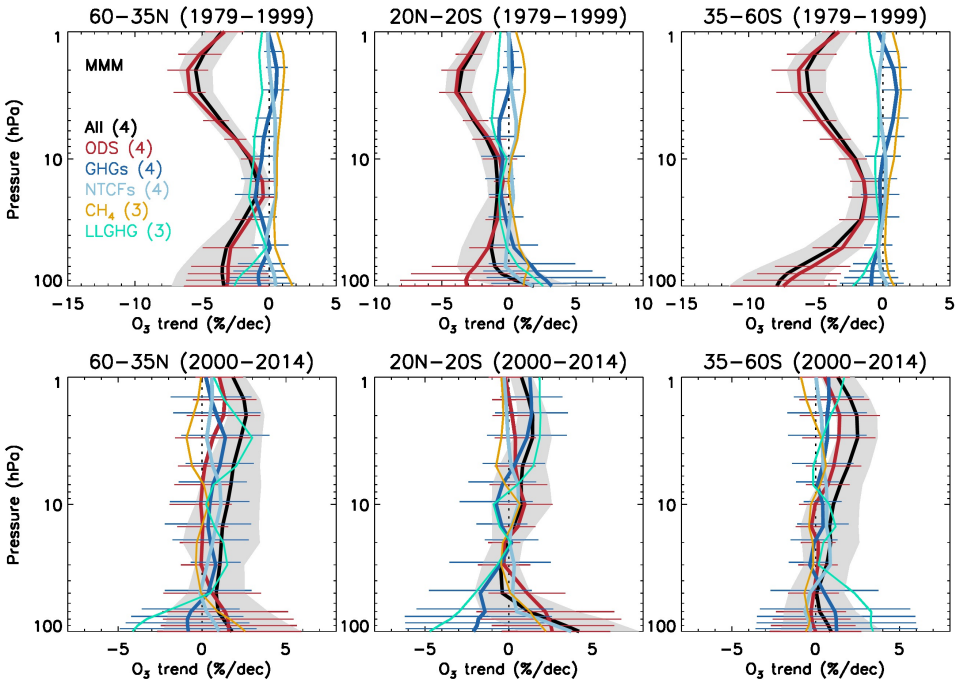

Figure 14. Multi-model mean vertically resolved stratospheric ozone trends (in %/decade) in the "all forcings" histSST simulation, and contributions from ODS, NTCFs, and GHGs (methane, N_2O and CO_2) for the periods of 1979-1999 (top panels) and 2000-2014 (bottom panels). Contributions from methane and LLGHGs (N_2O & CO_2) are also individually displayed in thinner lines. Numbers in brackets indicate the number of models included in the ensemble means. The Colour keys for each curve are displayed in the top left panel (black: all forcing; red: due to ODSs; dark blue: due to GHGs; light blue: due to NTCFs; orange: due to methane; cyan: due to LLGHGs). The grey filled region and horizontal lines are the uncertainty range in trends for all forcing, due to ODSs (red), and due to GHGs (dark blue), respectively. The 2σ uncertainty range accounts for a combination of model and statistical uncertainties.

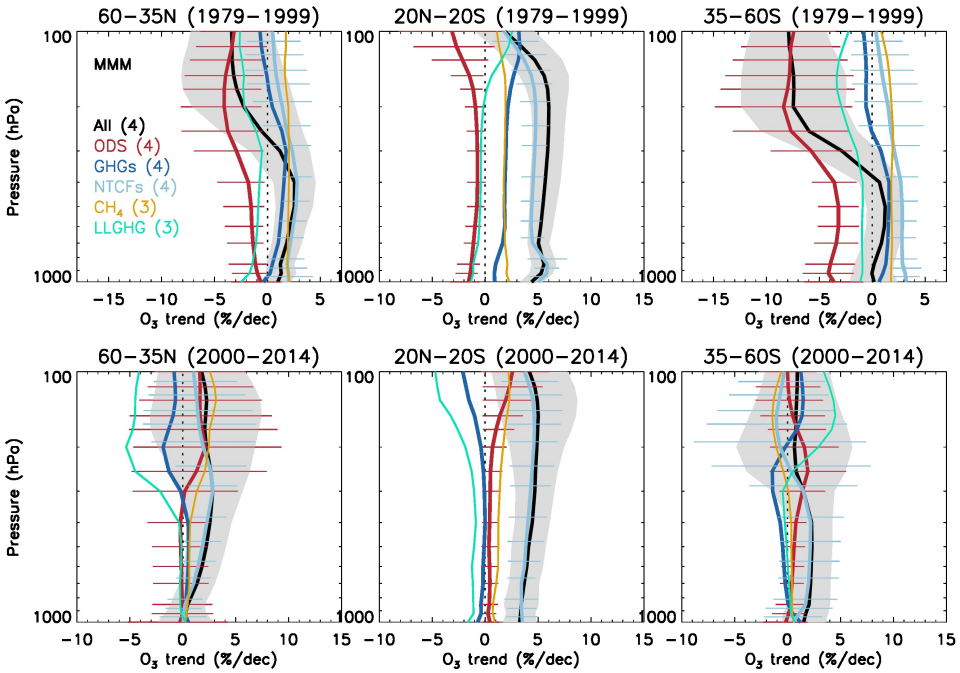

Figure 15. Same as Figure 14, but for the troposphere (1000 hPa - 100 hPa).

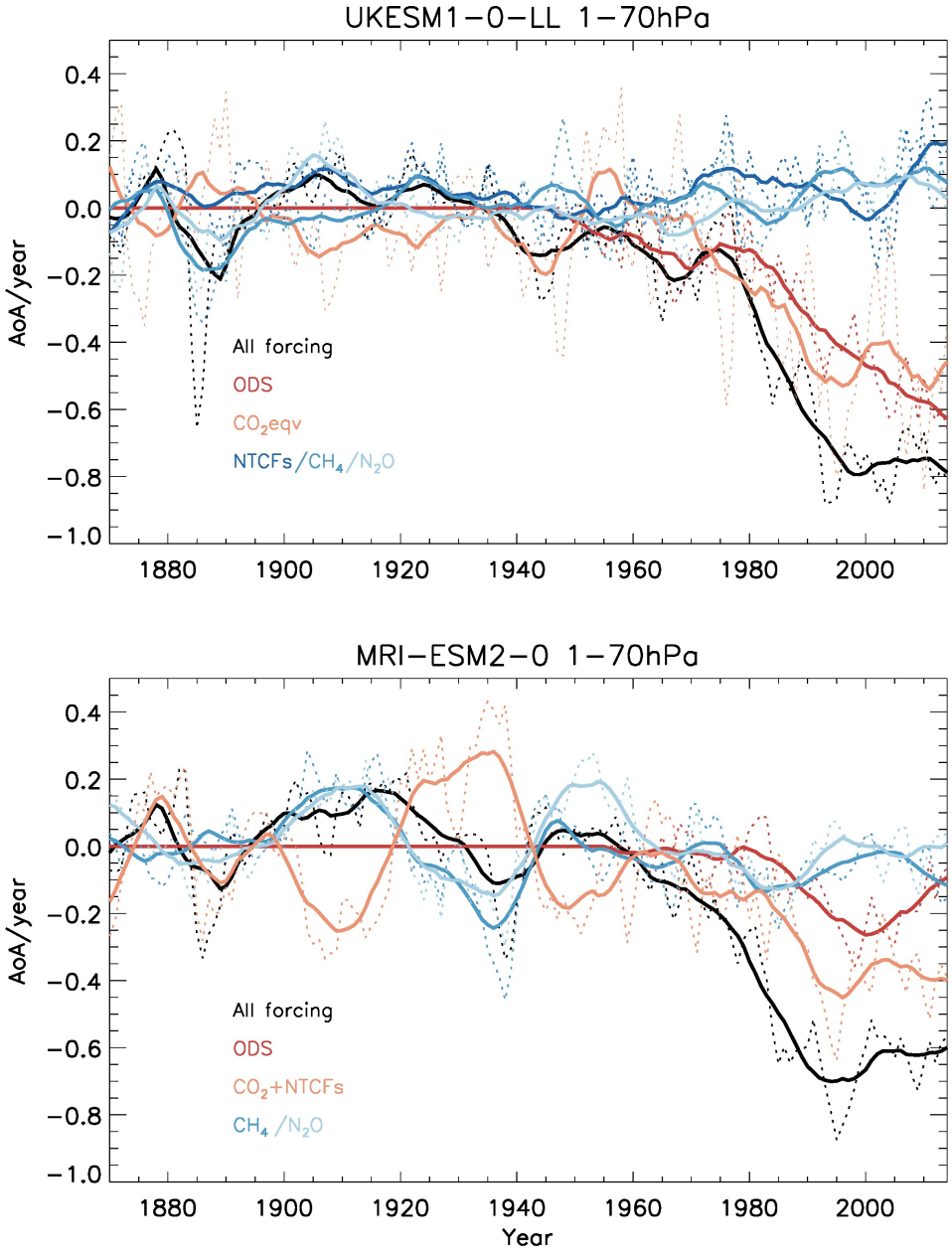

Figure 16. Changes in mean stratospheric age of air (in years, averaged between 70 and 1 hPa) from 1870 to 2014 from the "all forcings" histSST simulations and due to individual forcings in UKESM1-0-LL and MRI-ESM2-0. Solid think lines are the annual mean data smoothed using a 20-year boxcar filter. Dashed lines are the corresponding unfiltered annual mean data.

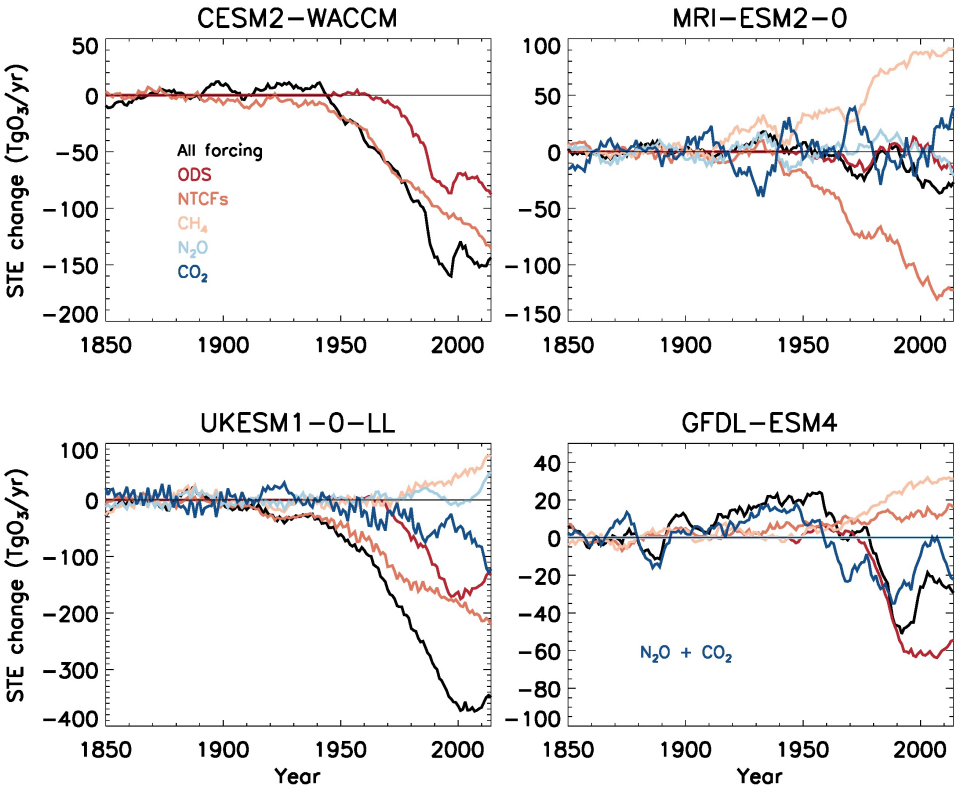

Figure 17. Changes in stratosphere-troposphere exchange (STE) of ozone in the "all forcings" histSST simulations and contributions due to individual forcings in four models (CESM2-WACCM, GFDL-ESM4, MRI-ESM2-0, and UKESM1-0-LL) over the period 1850-2014. Color keys are displayed in the top left panel (Black: all forcing; Colored lines are due to individual forcings: Red: ODSs; Dark orange: NTCFs; Light orange: methane; Light blue: N_2O; Dark blue: CO_2). STE is calculated as a residual between ozone production and loss in the troposphere. The tropopause is defined by the tropopause pressure calculated in each model using the WMO lapse rate definition as used by Griffiths et al. (2021). Annual mean data are smoothed using a 10-year boxcar filter.

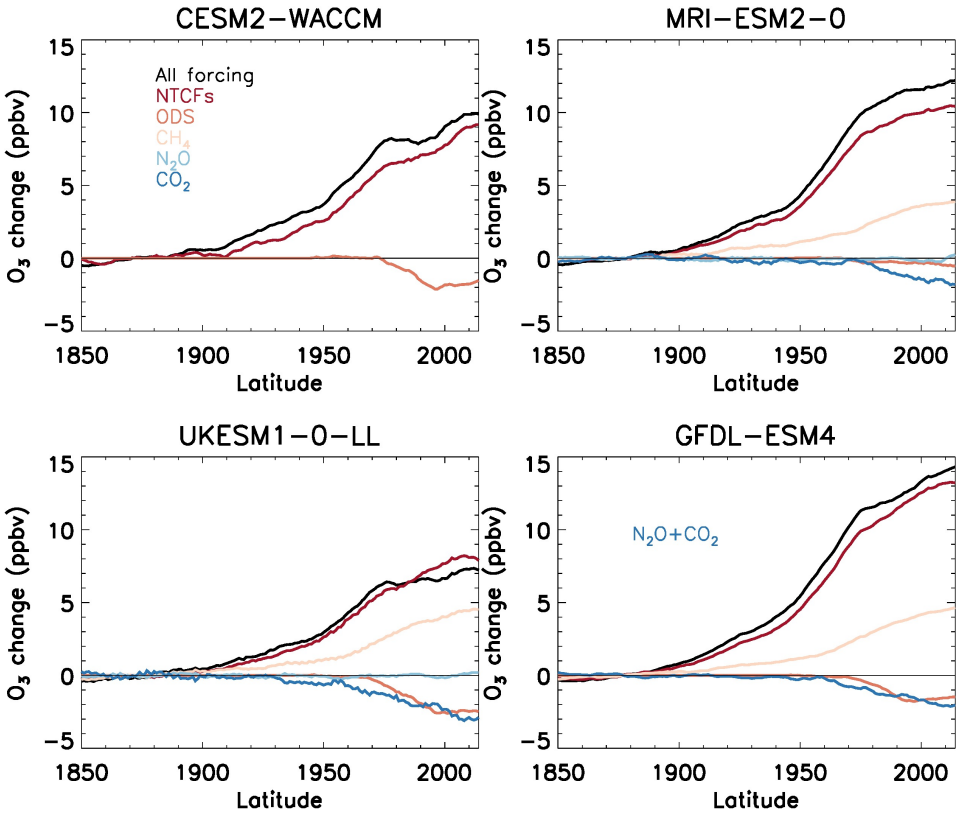

Figure 18. Changes in global mean near-surface ozone (ppbv) in "all forcings" histSST simulations and contributions to individual forcings over the period 1850-2014. Color keys are displayed in the top left panel (Black: all forcing; Colored lines are due to individual forcings: Red: ODSs; Dark orange: NTCFs; Light orange: methane; Light blue: N_2O; Dark blue: CO_2). In GFDL-ESM4, the impact of CO_2 includes N_2O as there is no separate N_2O perturbation simulation available. Annual mean data are smoothed using a 10-year boxcar filter.

Table 1. Models and simulations used in this study

Models	histSST	histSST-1950HC	histSST-piNTCF	histSST-piCH$_4$	histSST-piN$_2$O
CESM2-WACCM	x	x	x		
GFDL-ESM4	x	x	x	x	
MRI-ESM2-0	x	x	x	x	x
UKESM1-0-LL	x	x	x	x	x
GISS-E2-1-G	x	x	x	x	x
Model references					
CESM2-WACCM	Gettelman et al. (2019), Tilmes et al. (2019), Emmons et al. (2020), Danabasoglu et al. (2020)				
GFDL-ESM4	Horowitz et al. (2020), Dunne et al. (2020)				
MRI-ESM2-0	Deushi and Shibata (2011), Yukimoto et al. (2019)				
UKESM1-0-LL	Sellar et al. (2019), Archibald et al. (2020), Mulcahy et al. (2020)				
GISS-E2-1-G	Bauer et al. (2020), Kelley et al. (2020), Miller et al. (2021)				

Table 2. Derived ozone changes due to individual forcings

Models	ODS	NTCFs	CH_4	N_2O	CO_2	GHGs (CH_4, N_2O, CO_2)	LLGHGs (N_2O, CO_2)
CESM2-WACCM	x	x	x			x	
GFDL-ESM4	x	x	x			x	x
MRI-ESM2-0	x	x	x	x	x	x	x
UKESM1-0-LL	x	x	x	x	x	x	x
GISS-E2-1-G	x	x	x	x	x	x	x

$\Delta[O_3]_{ODS} = [O_3]_{histSST} - [O_3]_{histSST\text{-}1950HC}$

$\Delta[O_3]_{NTCF} = [O_3]_{histSST} - [O_3]_{histSST\text{-}piNTCF}$

$\Delta[O_3]_{CH_4} = [O_3]_{histSST} - [O_3]_{histSST\text{-}piCH_4}$

$\Delta[O_3]_{N_2O} = [O_3]_{histSST} - [O_3]_{histSST\text{-}piN_2O}$

$\Delta[O_3]_{CO_2} = [O_3]_{histSST} - \Delta[O_3]_{ODS} - \Delta[O_3]_{NTCF} - \Delta[O_3]_{CH_4} - \Delta[O_3]_{N_2O}$

$\Delta[O_3]_{GHGs} = [O_3]_{histSST} - \Delta[O_3]_{ODS} - \Delta[O_3]_{NTCF}$

$\Delta[O_3]_{LLGHGs} = \Delta[O_3]_{GHGs} - \Delta[O_3]_{CH_4}$

$[O_3]$ are timeseries of ozone concentrations, total- or partial columns from 1850 to 2014 in models expressed as deviations from the 1850-1900 average.

Acknowledgments

The authors acknowledge valuable comments on this manuscript by Douglas Kinnison. GZ and OM were supported by the NZ Government's Strategic Science Investment Fund (SSIF) through the NIWA programme CACV. JHTW acknowledges support by the Deep South National Science Challenge (DSNSC), funded by the New Zealand Ministry for Business, Innovation and Employment (MBIE). The authors acknowledge the contribution of NeSI high-performance computing facilities to the results of this research. New Zealand's national facilities are provided by the New Zealand eScience Infrastructure (NeSI) and funded jointly by NeSI's collaborator institutions and through MBIE's Research Infrastructure programme. JK and PTG were financially supported by NERC through NCAS (grant no. R8/H12/83/003). This work used Monsoon2, a collaborative High-Performance Computing facility funded by the Met Office and the Natural Environment Research Council, the NEXCS High-Performance Computing facility, funded by the Natural Environment Research Council and delivered by the Met Office between 2017 and 2021, and JASMIN, the UK collaborative data analysis facility. FOC was supported by the Met Office Hadley Centre Climate Program. NO and MD were supported by the Japan Society for the Promotion of Science KAKENHI (grant numbers: JP18H03363, JP18H05292, JP19K12312, JP20K04070 and JP21H03582), the Environment Research and Technology Development Fund (JPMEERF20202003 and JPMEERF20205001) of the Environmental Restoration and Conservation Agency of Japan, the Arctic Challenge for Sustainability II (ArCS II), Program Grant Number JPMXD1420318865, and a grant for the Global Environmental Research Coordination System from the Ministry of the Environment, Japan (MLIT1753). VN, LWH, and LTS thank the GFDL model development team and the leadership of NOAA/GFDL for their efforts and support in developing ESM4 as well as the GFDL modelling systems group and data portal team for technical support to make data available at the ESGF. The CESM project is supported primarily by the National Science Foundation (NSF). We thank all the scientists and software engineers who contributed to the development of CESM2. This material is based upon work supported by the National Center for Atmospheric Research, which is a major facility sponsored by the NSF under Cooperative Agreement No. 1852977. Computing and data storage resources, including the Cheyenne supercomputer (doi:10.5065/D6RX99HX), were provided by the Computational and Information Systems Laboratory (CISL) at NCAR. All CESM2 simulations presented here are freely available through the Climate Data Gate-

way (https://www.earthsystemgrid.org/). We acknowledge the World Climate Research Program, which, through its Working Group on Coupled Modeling, coordinated and promoted CMIP6. We thank the climate modeling groups for producing and making available their model output, the Earth System Grid Federation (ESGF) for archiving the data and providing access, and the multiple funding agencies who support CMIP6 and ESGF. All of the data from the CMIP and AerChemMIP simulations analysed in this study have been published on the Earth System Grid Federation (https://esgf-node.llnl.gov/search/cmip6/). We thank WOUDC for providing the groundbased total-column ozone data (https://woudc.org/archive/Projects-Campaigns/ZonalMeans/gb_1964-2017_za.txt).

References

Archibald, A. T., O'Connor, F. M., Abraham, N. L., Archer-Nicholls, S., Chipperfield, M. P., Dalvi, M., ... Zeng, G. (2020). Description and evaluation of the ukca stratosphere–troposphere chemistry scheme (strattrop vn 1.0) implemented in ukesm1. *Geoscientific Model Development*, *13*(3), 1223–1266. Retrieved from https://gmd.copernicus.org/articles/13/1223/2020/ doi: 10.5194/gmd-13-1223-2020

Bauer, S. E., Tsigaridis, K., Faluvegi, G., Kelley, M., Lo, K. K., Miller, R. L., ... Wu, J. (2020). Historical (1850–2014) aerosol evolution and role on climate forcing using the giss modele2.1 contribution to cmip6. *Journal of Advances in Modeling Earth Systems*, *12*(8), e2019MS001978. Retrieved from https://agupubs.onlinelibrary.wiley.com/doi/abs/10.1029/2019MS001978 (e2019MS001978 2019MS001978) doi: https://doi.org/10.1029/2019MS001978

Brasseur, G. P., & Solomon, S. (1984). *Aeronomy of the middle atmosphere: Chemistry and physics of the stratosphere and mesosphere* (2nd ed.). D. Reidel, Dordrecht, Holland.

Butchart, N. (2014). The brewer-dobson circulation. *Reviews of Geophysics*, *52*(2), 157-184. Retrieved from https://agupubs.onlinelibrary.wiley.com/doi/abs/10.1002/2013RG000448 doi: https://doi.org/10.1002/2013RG000448

Butchart, N., & Scaife, A. (2001). Removal of chlorofluorocarbons by increased mass exchange between the stratosphere and troposphere in a changing climate. *Na-*

ture, *410*, 799–802. Retrieved from https://doi.org/10.1038/35071047

Butler, A. H., Daniel, J. S., Portmann, R. W., Ravishankara, A. R., Young, P. J., Fahey, D. W., & Rosenlof, K. H. (2016, jun). Diverse policy implications for future ozone and surface UV in a changing climate. *Environmental Research Letters*, *11*(6), 064017. Retrieved from https://doi.org/10.1088/1748-9326/11/6/064017 doi: 10.1088/1748-9326/11/6/064017

Chipperfield, M. P., & Feng, W. (2003). Comment on: Stratospheric ozone depletion at northern mid-latitudes in the 21st century: The importance of future concentrations of greenhouse gases nitrous oxide and methane. *Geophysical Research Letters*, *30*(7). Retrieved from https://agupubs.onlinelibrary.wiley.com/doi/abs/10.1029/2002GL016353 doi: https://doi.org/10.1029/2002GL016353

Collins, W. J., Lamarque, J.-F., Schulz, M., Boucher, O., Eyring, V., Hegglin, M. I., ... Smith, S. J. (2017). AerChemMIP: Quantifying the effects of chemistry and aerosols in CMIP6. *Geoscientific Model Development*, *10*(2), 585–607. Retrieved from https://www.geosci-model-dev.net/10/585/2017/ doi: 10.5194/gmd-10-585-2017

Crutzen, P. J. (1970). The influence of nitrogen oxides on the atmospheric ozone content. *Quarterly Journal of the Royal Meteorological Society*, *96*(408), 320-325. Retrieved from https://rmets.onlinelibrary.wiley.com/doi/abs/10.1002/qj.49709640815 doi: https://doi.org/10.1002/qj.49709640815

Danabasoglu, G., Lamarque, J.-F., Bacmeister, J., Bailey, D. A., DuVivier, A. K., Edwards, J., ... Strand, W. G. (2020). The community earth system model version 2 (cesm2). *Journal of Advances in Modeling Earth Systems*, *12*(2), e2019MS001916. Retrieved from https://agupubs.onlinelibrary.wiley.com/doi/abs/10.1029/2019MS001916 (e2019MS001916 2019MS001916) doi: https://doi.org/10.1029/2019MS001916

Deushi, M., & Shibata, K. (2011). Development of a meteorological research institute chemistry-climate model version 2 for the study of tropospheric and stratospheric chemistry. *Papers in Meteorology and Geophysics*, *62*, 1-46. doi: 10.2467/mripapers.62.1

Dunne, J. P., Horowitz, L. W., Adcroft, A. J., Ginoux, P., Held, I. M., John, J. G., ... Zhao, M. (2020). The GFDL Earth System Model version 4.1 (GFDL-

ESM4.1): Overall coupled model description and simulation characteristics. *Journal of Advances in Modeling Earth Systems*, *12*, e2019MS002015. Retrieved from https://doi.org/10.1029/2019MS002015

Emmons, L. K., Schwantes, R. H., Orlando, J. J., Tyndall, G., Kinnison, D., Lamarque, J.-F., ... Pétron, G. (2020). The chemistry mechanism in the community earth system model version 2 (cesm2). *Journal of Advances in Modeling Earth Systems*, *12*(4), e2019MS001882. Retrieved from https://agupubs.onlinelibrary.wiley.com/doi/abs/10.1029/2019MS001882 (e2019MS001882 2019MS001882) doi: https://doi.org/10.1029/2019MS001882

Eyring, V., Arblaster, J. M., Cionni, I., Sedláček, J., Perlwitz, J., Young, P. J., ... Watanabe, S. (2013). Long-term ozone changes and associated climate impacts in cmip5 simulations. *Journal of Geophysical Research: Atmospheres*, *118*(10), 5029-5060. Retrieved from https://agupubs.onlinelibrary.wiley.com/doi/abs/10.1002/jgrd.50316 doi: https://doi.org/10.1002/jgrd.50316

Eyring, V., Bony, S., Meehl, G. A., Senior, C. A., Stevens, B., Stouffer, R. J., & Taylor, K. E. (2016). Overview of the Coupled Model Intercomparison Project Phase 6 (CMIP6) experimental design and organization. *Geoscientific Model Development*, *9*(5), 1937–1958. Retrieved from https://www.geosci-model-dev.net/9/1937/2016/ doi: 10.5194/gmd-9-1937-2016

Farman, G. B. G., J. C., & Shanklin, J. D. (1985). Large losses of total ozone in antarctica reveal seasonal clox/nox interaction. *Nature*, *315*. Retrieved from https://doi.org/10.1038/315207a0

Fioletov, V. E., Kerr, J. B., Hare, E. W., Labow, G. J., & McPeters, R. D. (1999). An assessment of the world ground-based total ozone network performance from the comparison with satellite data. *Journal of Geophysical Research: Atmospheres*, *104*(D1), 1737-1747. Retrieved from https://agupubs.onlinelibrary.wiley.com/doi/abs/10.1029/1998JD100046 doi: https://doi.org/10.1029/1998JD100046

Fleming, E. L., Jackman, C. H., Stolarski, R. S., & Douglass, A. R. (2011). A model study of the impact of source gas changes on the stratosphere for 1850–2100. *Atmospheric Chemistry and Physics*, *11*(16), 8515–8541. Retrieved from https://acp.copernicus.org/articles/11/8515/2011/ doi:

10.5194/acp-11-8515-2011

Gaudel, A., Cooper, O. R., Ancellet, G., Barret, B., Boynard, A., Burrows, J. P., ... Ziemke, J. (2018, 05). Tropospheric Ozone Assessment Report: Present-day distribution and trends of tropospheric ozone relevant to climate and global atmospheric chemistry model evaluation. *Elementa: Science of the Anthropocene*, *6*. Retrieved from https://doi.org/10.1525/elementa.291 (39) doi: 10.1525/elementa.291

Gettelman, A., Mills, M. J., Kinnison, D. E., Garcia, R. R., Smith, A. K., Marsh, D. R., ... Randel, W. J. (2019). The Whole Atmosphere Community Climate Model version 6 (WACCM6). *Journal of Geophysical Research: Atmospheres*, *124*(23), 12380-12403. Retrieved from https://agupubs.onlinelibrary.wiley.com/doi/abs/10.1029/2019JD030943 doi: 10.1029/2019JD030943

Griffiths, P. T., Murray, L. T., Zeng, G., Shin, Y. M., Abraham, N. L., Archibald, A. T., ... Zanis, P. (2021). Tropospheric ozone in cmip6 simulations. *Atmospheric Chemistry and Physics*, *21*(5), 4187–4218. Retrieved from https://acp.copernicus.org/articles/21/4187/2021/ doi: 10.5194/acp-21-4187-2021

Haigh, J. D., & Pyle, J. A. (1979). A two-dimensional calculation includingatmospheric carbon dioxide and stratospheric ozone.

Hegglin, S. T., M. (2009). Large climate-induced changes in ultraviolet index and stratosphere-to-troposphere ozone flux. *Nature Geosci*, *2*, 687–691. Retrieved from https://doi.org/10.1038/ngeo604

Horowitz, L. W., Naik, V., Paulot, F., Ginoux, P. A., Dunne, J. P., Mao, J., ... Zhao, M. (2020). The gfdl global atmospheric chemistry-climate model am4.1: Model description and simulation characteristics. *Journal of Advances in Modeling Earth Systems*, *12*(10), e2019MS002032. Retrieved from https://agupubs.onlinelibrary.wiley.com/doi/abs/10.1029/2019MS002032 (e2019MS002032 2019MS002032) doi: https://doi.org/10.1029/2019MS002032

Iglesias-Suarez, F., Young, P. J., & Wild, O. (2016). Stratospheric ozone change and related climate impacts over 1850–2100 as modelled by the ACCMIP ensemble. *Atmospheric Chemistry and Physics*, *16*(1), 343–363. Re-

trieved from https://acp.copernicus.org/articles/16/343/2016/ doi: 10.5194/acp-16-343-2016

Johnson, C. E., Collins, W. J., Stevenson, D. S., & Derwent, R. G. (1999). Relative roles of climate and emissions changes on future tropospheric oxidant concentrations. *Journal of Geophysical Research: Atmospheres*, *104*(D15), 18631-18645. Retrieved from https://agupubs.onlinelibrary.wiley.com/doi/abs/10.1029/1999JD900204 doi: https://doi.org/10.1029/1999JD900204

Keeble, J., Hassler, B., Banerjee, A., Checa-Garcia, R., Chiodo, G., Davis, S., ... Wu, T. (2021). Evaluating stratospheric ozone and water vapour changes in cmip6 models from 1850 to 2100. *Atmospheric Chemistry and Physics*, *21*(6), 5015–5061. Retrieved from https://acp.copernicus.org/articles/21/5015/2021/ doi: 10.5194/acp-21-5015-2021

Kelley, M., Schmidt, G. A., Nazarenko, L., Bauer, S. E., Ruedy, R., Russell, G. L., ... Yao, M. (2020). GISS-E2.1: Configurations and climatology. *Journal of Advances in Modelling Earth Systems*, *12*, e2019MS002025. Retrieved from https://doi.org/10.1029/2019MS002025

Li, F., Stolarski, R. S., & Newman, P. A. (2009). Stratospheric ozone in the post-cfc era. *Atmospheric Chemistry and Physics*, *9*(6), 2207–2213. Retrieved from https://acp.copernicus.org/articles/9/2207/2009/ doi: 10.5194/acp-9-2207-2009

Meinshausen, M., Vogel, E., Nauels, A., Lorbacher, K., Meinshausen, N., Etheridge, D. M., ... Weiss, R. (2017). Historical greenhouse gas concentrations for climate modelling (CMIP6). *Geoscientific Model Development*, *10*, 2057–2116. Retrieved from https://doi.org/10.5194/gmd-10-2057-2017 doi: 10.5194/gmd-10-2057-2017

Miller, R. L., Schmidt, G. A., Nazarenko, L., Bauer, S. E., Kelley, M., Ruedy, R., ... Yao, M.-S. (2021). Cmip6 historical simulations (1850-2014) with giss-e2.1. *J. Adv. Model. Earth Syst.*, *13*(1), e2019MS002034. doi: 10.1029/2019MS002034

Morgenstern, O. (2021). The Southern Annular Mode in 6$^{\text{th}}$ Coupled Model Intercomparison Project models. *Journal of Geophysical Research: Atmospheres*, *126*(5), e2020JD034161. Retrieved from https://agupubs.onlinelibrary.wiley.com/doi/abs/10.1029/2020JD034161 doi: 10.1029/2020JD034161

Morgenstern, O., O'Connor, F. M., Johnson, B. T., Zeng, G., Mulcahy, J. P.,

Williams, J., ... Kinnison, D. E. (2020). Reappraisal of the climate impacts of ozone-depleting substances. *Geophysical Research Letters*, *47*(20), e2020GL088295. Retrieved from https://agupubs.onlinelibrary.wiley.com/doi/abs/10.1029/2020GL088295 doi: 10.1029/2020GL088295

Morgenstern, O., Stone, K. A., Schofield, R., Akiyoshi, H., Yamashita, Y., Kinnison, D. E., ... Chipperfield, M. P. (2018). Ozone sensitivity to varying greenhouse gases and ozone-depleting substances in CCMI-1 simulations. *Atmospheric Chemistry and Physics*, *18*, 1091–1114. Retrieved from https://doi.org/10.5194/acp-18-1091-2018

Mulcahy, J. P., Johnson, C., Jones, C. G., Povey, A. C., Scott, C. E., Sellar, A., ... Yool, A. (2020). Description and evaluation of aerosol in ukesm1 and hadgem3-gc3.1 cmip6 historical simulations. *Geoscientific Model Development*, *13*(12), 6383–6423. Retrieved from https://gmd.copernicus.org/articles/13/6383/2020/ doi: 10.5194/gmd-13-6383-2020

Newman, P. A., Daniel, J. S., Waugh, D. W., & Nash, E. R. (2007). A new formulation of equivalent effective stratospheric chlorine (EESC). *Atmospheric Chemistry and Physics*, *7*(17), 4537–4552. Retrieved from https://acp.copernicus.org/articles/7/4537/2007/ doi: 10.5194/acp-7-4537-2007

Oberländer-Hayn, S., Gerber, E. P., Abalichin, J., Akiyoshi, H., Kerschbaumer, A., Kubin, A., ... Oman, L. D. (2016). Is the brewer-dobson circulation increasing or moving upward? *Geophysical Research Letters*, *43*(4), 1772-1779. Retrieved from https://agupubs.onlinelibrary.wiley.com/doi/abs/10.1002/2015GL067545 doi: https://doi.org/10.1002/2015GL067545

Oman, L. D., Plummer, D. A., Waugh, D. W., Austin, J., Scinocca, J. F., Douglass, A. R., ... Ziemke, J. R. (2010). Multimodel assessment of the factors driving stratospheric ozone evolution over the 21st century. *Journal of Geophysical Research: Atmospheres*, *115*(D24). Retrieved from https://agupubs.onlinelibrary.wiley.com/doi/abs/10.1029/2010JD014362 doi: https://doi.org/10.1029/2010JD014362

Polvani, L. M., Wang, L., Abalos, M., Butchart, N., Chipperfield, M. P., Dameris, M., ... Stone, K. A. (2019). Large impacts, past and future, of ozone-depleting substances on brewer-dobson circulation trends: A multimodel assessment. *Journal of Geophysical Research: Atmospheres*, *124*(13), 6669-

6680. Retrieved from https://agupubs.onlinelibrary.wiley.com/doi/abs/10.1029/2018JD029516 doi: https://doi.org/10.1029/2018JD029516

Portmann, R. W., Daniel, J. S., & Ravishankara, A. R. (2012). Stratospheric ozone depletion due to nitrous oxide: influences of other gases. *Philosophical Transactions of the Royal Society B: Biological Sciences*, *367*(1593), 1256-1264. Retrieved from https://royalsocietypublishing.org/doi/abs/10.1098/rstb.2011.0377 doi: 10.1098/rstb.2011.0377

Ravishankara, A. R., Daniel, J. S., & Portmann, R. W. (2009). Nitrous oxide (n¡sub¿2¡/sub¿o): The dominant ozone-depleting substance emitted in the 21st century. *Science*, *326*(5949), 123-125. Retrieved from https://www.science.org/doi/abs/10.1126/science.1176985 doi: 10.1126/science.1176985

Reader, M. C., Plummer, D. A., Scinocca, J. F., & Shepherd, T. G. (2013). Contributions to twentieth century total column ozone change from halocarbons, tropospheric ozone precursors, and climate change. *Geophysical Research Letters*, *40*(23), 6276-6281. Retrieved from https://agupubs.onlinelibrary.wiley.com/doi/abs/10.1002/2013GL057776 doi: https://doi.org/10.1002/2013GL057776

Revell, L. E., Bodeker, G. E., Smale, D., Lehmann, R., Huck, P. E., Williamson, B. E., ... Struthers, H. (2012). The effectiveness of n2o in depleting stratospheric ozone. *Geophysical Research Letters*, *39*(15). Retrieved from https://agupubs.onlinelibrary.wiley.com/doi/abs/10.1029/2012GL052143 doi: https://doi.org/10.1029/2012GL052143

Revell, L. E., Tummon, F., Salawitch, R. J., Stenke, A., & Peter, T. (2015). The changing ozone depletion potential of n2o in a future climate. *Geophysical Research Letters*, *42*(22), 10,047-10,055. Retrieved from https://agupubs.onlinelibrary.wiley.com/doi/abs/10.1002/2015GL065702 doi: https://doi.org/10.1002/2015GL065702

Sellar, A. A., Jones, C. G., Mulcahy, J. P., Tang, Y., Yool, A., Wiltshire, A., ... Zerroukat, M. (2019). UKESM1: Description and evaluation of the U.K. Earth System Model. *Journal of Advances in Modeling Earth Systems*, *11*(12), 4513-4558. Retrieved from https://agupubs.onlinelibrary.wiley.com/doi/abs/10.1029/2019MS001739 doi: 10.1029/2019MS001739

Shepherd, T. G. (2008). Dynamics, stratospheric ozone, and climate change. *Atmosphere-Ocean*, *46*(1), 117-138. Retrieved from https://doi.org/10.3137/ao.460106 doi: 10.3137/ao.460106

Solomon, S. (1999). Stratospheric ozone depletion: A review of concepts and history. *Reviews of Geophysics*, *37*(3), 275-316. Retrieved from https://agupubs.onlinelibrary.wiley.com/doi/abs/10.1029/1999RG900008 doi: https://doi.org/10.1029/1999RG900008

Stevenson, D. S., Dentener, F. J., Schultz, M. G., Ellingsen, K., van Noije, T. P. C., Wild, O., ... Szopa, S. (2006). Multimodel ensemble simulations of present-day and near-future tropospheric ozone. *Journal of Geophysical Research: Atmospheres*, *111*(D8). Retrieved from https://agupubs.onlinelibrary.wiley.com/doi/abs/10.1029/2005JD006338 doi: https://doi.org/10.1029/2005JD006338

Stevenson, D. S., Zhao, A., Naik, V., O'Connor, F. M., Tilmes, S., Zeng, G., ... Emmons, L. (2020). Trends in global tropospheric hydroxyl radical and methane lifetime since 1850 from aerchemmip. *Atmospheric Chemistry and Physics*, *20*(21), 12905–12920. Retrieved from https://acp.copernicus.org/articles/20/12905/2020/ doi: 10.5194/acp-20-12905-2020

Stolarski, D. A. R. O. L. D., R. S., & Waugh, D. W. (2015). Impact of future nitrous oxide and carbon dioxide emissions on the stratospheric ozone layer. *Environ. Res. Lett.*, *10*(034011). Retrieved from https://doi.org/10.1088/1748-9326/10/3/034011

Tarasick, D., Carey-Smith, T., Hocking, W., Moeini, O., He, H., Liu, J., ... Merrill, J. (2019). Quantifying stratosphere-troposphere transport of ozone using balloon-borne ozonesondes, radar windprofilers and trajectory models. *Atmospheric Environment*, *198*, 496-509. Retrieved from https://www.sciencedirect.com/science/article/pii/S1352231018307301 doi: https://doi.org/10.1016/j.atmosenv.2018.10.040

Tilmes, S., Hodzic, A., Emmons, L. K., Mills, M. J., Gettelman, A., Kinnison, D. E., ... Liu, X. (2019). Climate forcing and trends of organic aerosols in the community earth system model (cesm2). *Journal of Advances in Modeling Earth Systems*, *11*(12), 4323-4351. Retrieved from https://agupubs.onlinelibrary.wiley.com/doi/abs/10.1029/2019MS001827 doi:

https://doi.org/10.1029/2019MS001827

Volz, A., & Kley, D. (1988). Evaluation of the montsouris series of ozone measurements made in the nineteenth century. *Nature*, *332*. doi: doi:10.1038/332240a0

WMO. (2018). *Scientific Assessment of Ozone Depletion: 2018*. Geneva, Switzerland: World Meteorological Organization. Retrieved from `https://www.esrl.noaa.gov/csl/assessments/ozone/2018/`

Young, P. J., Archibald, A. T., Bowman, K. W., Lamarque, J.-F., Naik, V., Stevenson, D. S., ... Zeng, G. (2013). Pre-industrial to end 21st century projections of tropospheric ozone from the atmospheric chemistry and climate model intercomparison project (accmip). *Atmospheric Chemistry and Physics*, *13*(4), 2063–2090. Retrieved from `https://acp.copernicus.org/articles/13/2063/2013/` doi: 10.5194/acp-13-2063-2013

Yukimoto, S., Kawai, H., Koshiro, T., Oshima, N., Yoshida, K., Urakawa, S., ... ISHII, M. (2019). The Meteorological Research Institute Earth System Model Version 2.0, MRI-ESM2.0: Description and basic evaluation of the physical component. *Journal of the Meteorological Society of Japan Ser. II*. doi: 10.2151/jmsj.2019-051

Zeng, G., Morgenstern, O., Braesicke, P., & Pyle, J. A. (2010). Impact of stratospheric ozone recovery on tropospheric ozone and its budget. *Geophysical Research Letters*, *37*(9). Retrieved from `https://agupubs.onlinelibrary.wiley.com/doi/abs/10.1029/2010GL042812` doi: https://doi.org/10.1029/2010GL042812